



Contents lists available at ScienceDirect

Bioorganic Chemistry

journal homepage: www.elsevier.com/locate/bioorg

Discovery of 4-((4-(4-(3-(2-(2,6-difluorophenyl)-4-oxothiazolidin-3-yl)ureido)-2-fluorophenoxy)-6-methoxyquinolin-7-yl)oxy)-N,N-diethylpiperidine-1-carboxamide as kinase inhibitor for the treatment of colorectal cancer

Yuting Zhou, Xingwei Xu, Fei Wang, Huan He^{*}, Baohui Qi^{*}

Department of Bioengineering, Zhuhai Campus of Zunyi Medical University, Zhuhai 519041, Guangdong Province, China

ARTICLE INFO

Keywords:

Design
Synthesis
Thiazolidinone
Quinoline
Tyrosine kinase inhibitors
Colorectal cancer

ABSTRACT

In this study, a novel series of 4,6,7-trisubstituted quinoline analogues bearing thiazolidinones were designed and synthesized based on our previous study. Among them, the most potent compound **15i**, 4-((4-(4-(3-(2-(2,6-difluorophenyl)-4-oxothiazolidin-3-yl)ureido)-2-fluorophenoxy)-6-methoxyquinolin-7-yl)oxy)-N,N-diethylpiperidine-1-carboxamide was identified as a multi-kinase inhibitor. The results of MTT assay revealed *in vitro* anti-tumor activities against HT-29 cells of compound **15i** with an IC₅₀ value of 0.19 μM which was 14.5-fold more potent than that of Regorafenib. In the cellular context, significant antiproliferation, cytotoxicity and induction of apoptosis on HT-29 cells in a dose- and time-dependent manner were confirmed by IncuCyte live-cell imaging assays. Moreover, compound **15i** strongly induced apoptosis by arresting cell cycle into the G2/M phase. No antiproliferation and cytotoxicity against human normal colorectal mucosa epithelial cell FHC was observed at 10.0 μg/mL or lower concentrations which indicated that the toxicity to normal cells of compound **15i** was much lower than that of Regorafenib. Based on the above findings, further structural modification will be conducted for the development of more potent kinase inhibitors as anticancer agents.

1. Introduction

Receptor tyrosine kinases (RTKs) has attracted considerable interest as therapeutic targets for numerous cancers due to their regulation of cell survival, proliferation, migration and angiogenesis in cancer development and metastasis [1]. Mesenchymal-epithelial transition factor (c-Met), also known as a receptor for hepatocyte growth factor/scatter factor (HGF/SF), is one of the key members of RTKs [2]. Phosphorylated c-Met is responsible for triggering the activation of its downstream signaling pathways that regulate specific biological events, such as mitogen-activated protein kinases (MAPKs), phosphoinositide 3-kinase/protein kinase B (PI3K/Akt), signal transducer and activator of transcription proteins (STAT), and nuclear factor-κB (NF-κB) pathways, etc. [3,4]. In a variety of cancer cells, overexpression and/or mutation of c-Met are associated with cell growth, invasion, proliferation, and protection from apoptosis, poor prognosis, etc. [5–9]. Récepteur d'Origine Nantais (Ron) is the only other member of c-Met family and normally expressed at low level in epithelial cells. The structures of Ron and c-Met

share 34% overall homology and the tyrosine kinase region of both receptors share 80% homology [10,11]. The phosphorylated Ron can activate a great number of transduction proteins and trigger its downstream signaling cascades, including c-Src, β-catenin/TCF-4, ERK1/2, MAPKs, SMAD/TGF-β, JNK/STAT, and PI3K/AKT, etc. [12–14]. In addition, the MSP/Ron signaling pathway has been implicated in tumorigenic activities and malignant progression [15,16].

Therefore, Ron and c-Met kinases have been extensively studied as targets of anticancer drugs, and a great deal of kinase inhibitors have been studied in clinical trial stage or used for cancer treatment in the clinic, such as Merestinib (1), Cabozantinib (2), MK-8033 (3), Nimgetinib (4) and Altiratinib (5) (Fig. 1) [17–21]. Unfortunately, the majority of studies were limited to *in vitro* experiments due to their unfavorable pharmacologic and/or pharmacokinetic properties, as well as intolerable toxicity. Thus, a series of novel quinoline analogues bearing thiazolidinone moieties as c-Met/Ron dual inhibitors were studied in the present work.

In our previous study, *N*¹-(4-((7-(3-(4-ethylpiperazin-1-yl)propoxy)-

^{*} Corresponding author.

E-mail addresses: hehuan_1029@163.com (H. He), bhqi@zmu.gd.cn (B. Qi).

<https://doi.org/10.1016/j.bioorg.2020.104511>

Received 28 June 2020; Received in revised form 1 October 2020; Accepted 19 November 2020

Available online 24 November 2020

0045-2068/© 2020 Elsevier Inc. All rights reserved.

6-methoxyquinolin-4-yl)oxy)-3,5-difluorophenyl)- N^3 -(2-(2,6-difluorophenyl)-4-oxothiazolidin-3-yl)urea (**EJMECH-19a**) was discovered as a multi-kinase inhibitor with IC_{50} values of 15.0 nM and 2.9 nM against c-Met and Ron, respectively (Fig. 2) [22]. The biological results indicated that it was a potent anticancer agent against several cancer cell lines, especially human colorectal carcinoma cell line HT-29 (IC_{50} = 0.073 μ M). Preliminary study of SARs indicated that the terminal heterocycles at 7-position of quinoline was a potential group to improve the anticancer activity and the aqueous solubility (Fig. 2). More importantly, the nitrogen atom of quinoline and the thiazolidinone urea moiety could form three strong H-bonds with Met1160, Lys1110 and Glu1127 [22,23].

Based on the above biological results and obtained SARs in our previous studies, a hydrophilic piperidine fragment (part I) was introduced into the quinoline ring according to the structure of Vandetanib (Fig. 2). In addition, the central phenyl ring (A ring) and the thiazolidinone urea moiety were also investigated in this work. Moreover, detailed structure-activity relationships (SARs), docking studies, cytotoxicity against normal cells and preliminary antitumor mechanism were presented meantime.

2. Chemistry

Compounds **15a-j** were obtained by the general approach outlined in Scheme 1. Commercially available 7-(benzyloxy)-4-chloro-6-methoxyquinoline was used as starting material to synthesize 4-arylquinolines **6a-c** via substitution of chloride with 4-nitrophenol, 2-fluoro-4-nitrophenol or 3-fluoro-4-nitrophenol under reflux in PhCl. Intermediates **6a-c** were converted to phenols **7a-c** by stirring in HBr at room temperature [24]. Nucleophilic substitution was used to convert **7a-c** to intermediates **8a-c** in DMF containing Cs_2CO_3 [25]. Piperidine derivatives **9a-c** were afforded by deprotection of the *N*-Boc group by CF_3COOH in CH_2Cl_2 . Reaction of intermediates **9a-c** with the correspond acyl chlorides or sulfonyl chlorides in CH_2Cl_2 provided the desired **10a-j** in high yields. Reduction of **10a-j** by powdered iron in 90% EtOH to afford amines **11a-j**. Intermediates **11a-j** were reacted with phenyl chloroformate in the presence of pyridine to produce **13a-j**, followed by hydrazinolysis reaction with 80% hydrazine hydrate in xylene with vigorous agitation. Semicarbazones **14a-j** were obtained by

condensation of **13a-j** with 2,6-difluorobenzaldehyde in favor of catalytic HOAc in *i*-PrOH. Finally, the target 4-oxothiazolidine derivatives **15a-j** were afforded by cyclization with mercaptoacetic acid in the presence of $SiCl_4$ [22].

Target compound **25**, 4-((4-(3-(3-(2-(2,6-difluorophenyl)-4-oxothiazolidin-3-yl)ureido)phenoxy)-6-methoxyquinolin-7-yl)oxy)-*N,N*-diethylpiperidine-1-carboxamide, was prepared by similar synthetic routes (Scheme 2).

3. Results and discussion

3.1. Structure-Activity relationship

Our previous efforts indicated that the quinoline derivatives bearing thiazolidinone fragments showed potent *in vitro* kinase inhibitory activity against c-Met/Ron and anticancer activity against various cancer cell lines, especially human colorectal cancer cell line HT-29 [22]. Thus, taking Regorafenib treatment for metastatic colorectal cancer (mCRC) in clinic as positive control, preliminary *in vitro* anticancer activity of all newly synthesized compounds against HT-29 cells was determined in this study. The inhibitory potency against c-Met, Ron and HT-29 cells were all shown in Table 1.

At the beginning of our work, compounds **15a-d** with diversified acyl groups at nitro atoms of piperidine rings were synthesized and evaluated for their biological activity. Among them, diethylcarbamyloxy analogue **15c** showed potent *in vitro* antitumor activity (HT-29 IC_{50} = 0.61 μ M) and kinase inhibitory activity. The results indicated that the introduction of an additional nitro atom might be beneficial for biological activity. Moreover, the more steric and hydrophobic analogues **15a** and **15b** showed lower potency in c-Met inhibitory rate and *in vitro* antitumor activity.

Subsequently, compounds bearing substituted sulfonyl groups (**15e-h**) were explored. As a general trend, the sulfonyl analogues were not well tolerated according to their biological activity, especially thiophen-2-ylsulfonyl compound **15h**. The above results indicated that bulky effect likely had some effect on the potency.

Moving the thiazolidinone urea moiety to the 3-position of central phenyl ring A (**25**) led to a significant decrease in potency against both kinases compared to compound **15c**. Docking study indicated that a

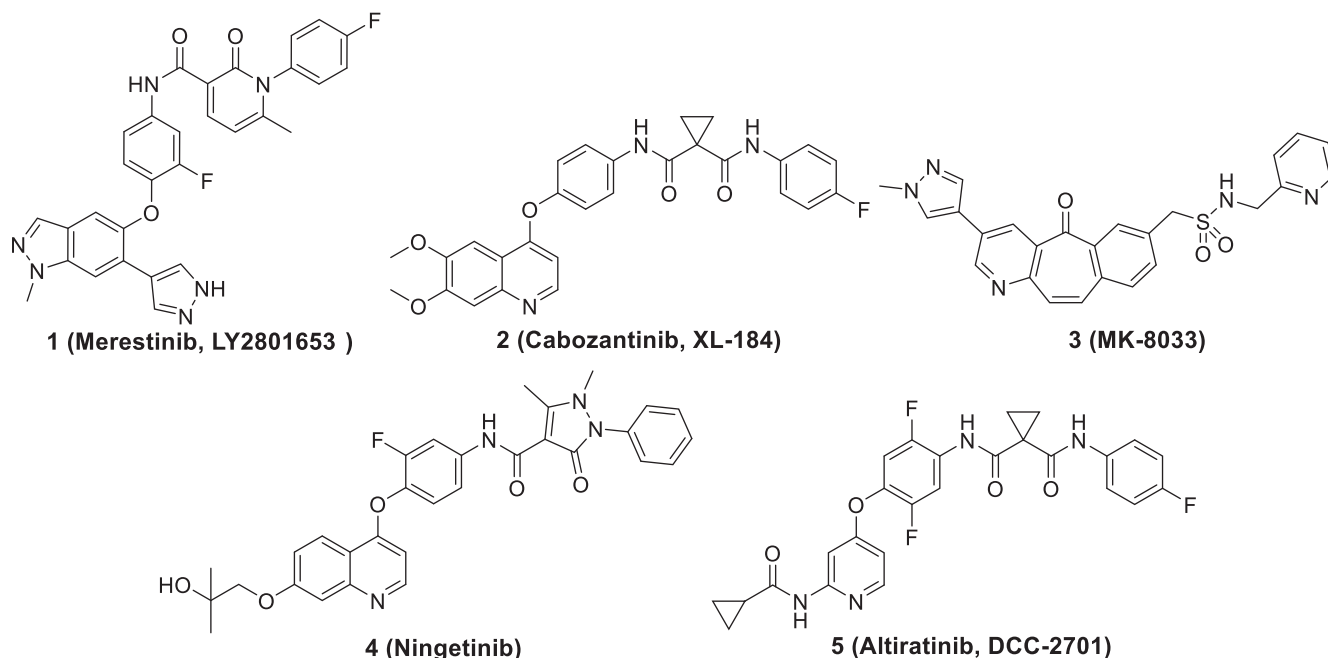


Fig. 1. The representative c-Met and/or Ron inhibitors.

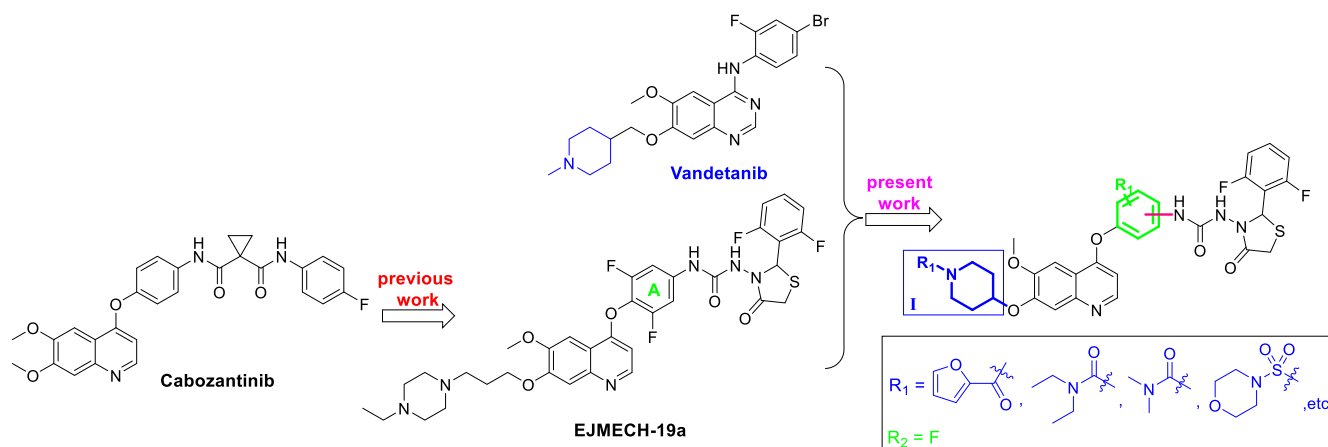
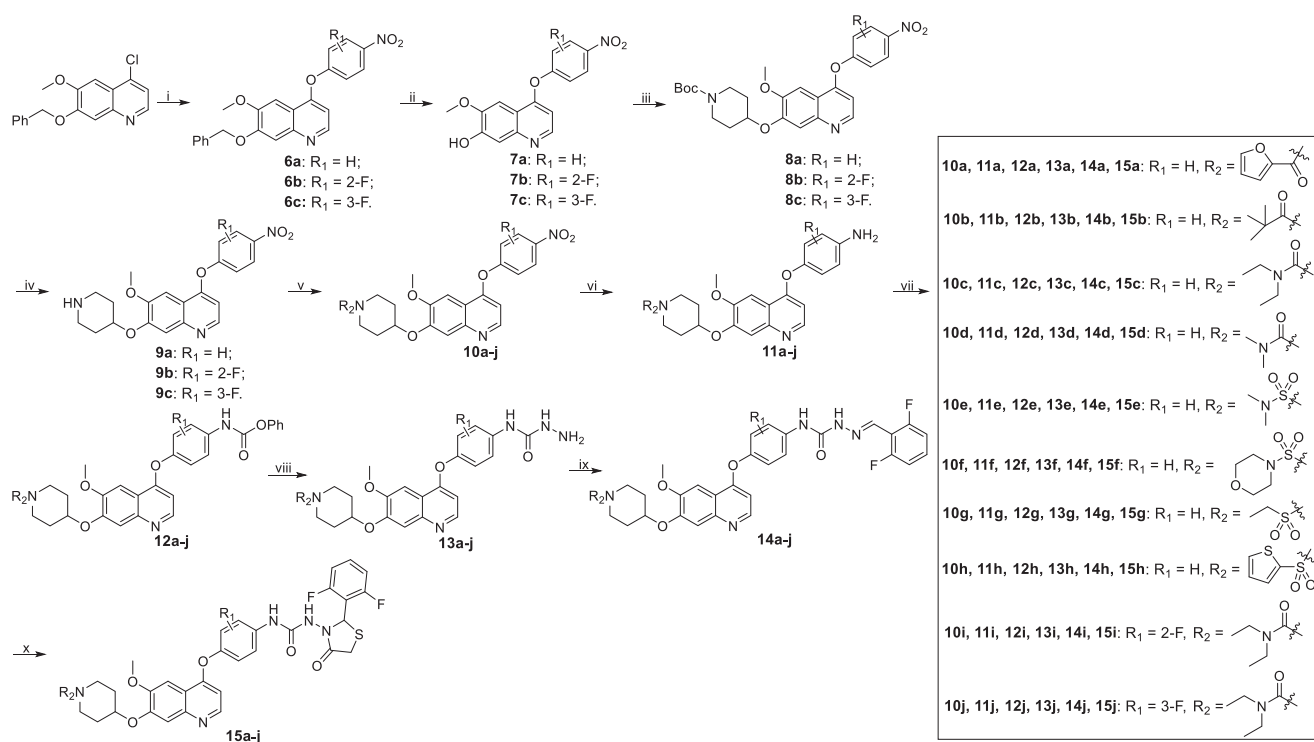


Fig. 2. Our previous work and the design of novel compounds in the present work.



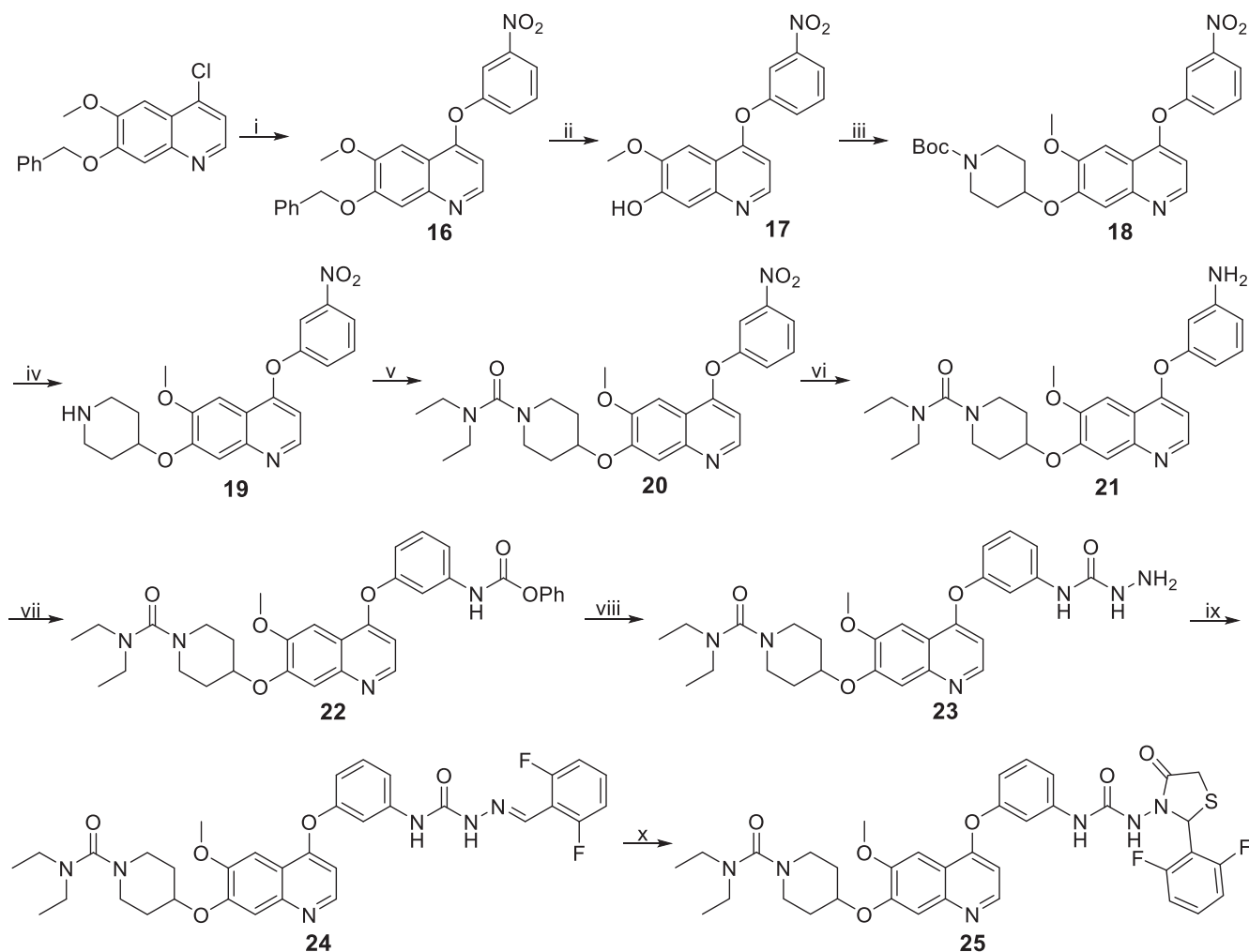
Scheme 1. Synthesis of target compounds 15a-j. Reagents and conditions: i) 4-nitrophenol (6a), 2-fluoro-4-nitrophenol (6b) or 3-fluoro-4-nitrophenol (6c), PhCl, reflux, 16 h; ii) 33% HBr in HOAc, rt, 3 h; iii) 1-Boc-4-methanesulfonyloxypiperidine, Cs₂CO₃, DMF, 110 °C, 6 h; iv) CF₃COOH, CH₂Cl₂, rt, 2 h; v) acyl chlorides or sulfonyl chlorides, Et₃N, CH₂Cl₂, rt, 4–5 h; vi) Fe, 90% EtOH, HCl, reflux, 4–6 h; vii) phenyl chloroformate, pyridine, CH₂Cl₂, rt, 2 h; viii) 80% hydrazine hydrate, xylene, 70 °C, 2 h; ix) 2,6-difluorobenzaldehyde, *i*-PrOH, HOAc (cat.), reflux, 2 h; x) mercaptoacetic acid, SiCl₄, CH₂Cl₂, reflux, 6 h.

significant H-bond formed by oxygen atom in urea fragment with the residue of Lys1110 vanished which led to the decrease in potency (Fig. 4).

Having identified well tolerated group on R₂ and the position of thiazolidinone urea moiety, the modification came to the R₁ and compounds 15i and 15j were prepared. Based on our previous work, only fluorine atom was introduced in this work. As shown in Table 1, the introduction of fluorine atom on the phenyl ring A (Fig. 2) resulted a boost in both kinase inhibitory rate and *in vitro* antitumor activity. The 2-fluoro analogue 15i (HT-29 IC₅₀ = 0.19 μM) displayed an over 3-fold increase in antitumor activity than that of compound 15c (HT-29 IC₅₀ = 0.61 μM). In addition, the biological results also suggested that 2-fluoro analogue 15i was superior to 3-fluoro analogue 15j.

3.2. Molecular docking study

Docking studies of the most potent compound 15i and Cabozantinib was performed by Molecular Operating Environment 2018.01 (Chemical Computing Group ULC, Montreal, QC, Canada). As could be seen in Fig. 3B and C, compound 15i adopted an extended conformation as type II kinase inhibitor Cabozantinib [26]. The results of docking study indicated that the S values of compound 15i and Cabozantinib were -11.7295 and -11.9807, respectively. Two canonical H-bonds were formed by nitrogen atom in quinoline and oxygen atom in urea fragment with Met1160 and Lys1110, respectively. The hydrophobic pocket formed by the residues of Phe1134, Phe1200, Ile1130 and Ala1221 was occupied by the terminal 2,6-difluorophenyl ring, and weak H-arene interaction was formed by 2,6-difluorophenyl fragment with Phe1134.



Scheme 2. Synthesis of target compound **25**. Reagents and conditions: i) 3-nitrophenol, reflux, 18 h; ii) 33% HBr in HOAc, rt, 3 h; iii) 1-Boc-4-methanesulfonylpiperidine, Cs₂CO₃, DMF, 110 °C, 6 h; iv) CF₃COOH, CH₂Cl₂, rt, 2 h; v) diethylcarbamic chloride, Et₃N, CH₂Cl₂, rt, 5 h; vi) Fe, 90% EtOH, conc. HCl, reflux, 4 h; vii) phenyl chloroformate, pyridine, CH₂Cl₂, rt, 2 h; viii) 80% hydrazine hydrate, xylene, 70 °C, 2 h; ix) 2,6-difluorobenzaldehyde, *i*-PrOH, HOAc (cat.), reflux, 2 h; x) mercaptoacetic acid, SiCl₄, CH₂Cl₂, reflux, 6 h.

In order to further clarify SAR, the study of molecular superposition was conducted. The results indicated that compounds **15c** and **15i** were well embedded in the binding pocket by similar alignment (Fig. 4). Moving the 2-(2,6-difluorophenyl)-4-oxothiazolidin-3-ylureido fragment to the 3-position of central phenyl ring (**25**) led to the disappearance of a strong H-bond formed with the residue of Lys1110. Thus, the change of binding mode might be responsible for the dramatic decrease in kinase inhibitory activity.

3.3. IncuCyte live-cell imaging assays

Taking Regorafenib as positive control, antiproliferation and cytotoxicity against HT-29 cells and human normal colorectal mucosa epithelial FHC cells were determined by IncuCyte live-cell imaging assays.

3.3.1. Cytotoxicity and antiproliferation against HT-29 cells

The kinetics of antiproliferation and cytotoxicity of compound **15i** and Regorafenib were evaluated by IncuCyte live-cell imaging assays. As indicated in Figs. 5A and 6, at the concentration of 5.0 µg/mL, 0.56 µg/mL and 0.19 µg/mL, compound **15i** could significantly induce cytotoxicity after treatment for 36 h. No cytotoxicity could be seen by treatment with 5.0 µg/mL of Regorafenib. Moreover, a significant reduction in cell proliferation induced by compound **15i** was observed which was

inferior to that of Regorafenib at the same concentration. The above results indicated that compound **15i** could induce considerable antiproliferation and cytotoxicity in a dose- and time-dependent manner.

3.3.2. Antiproliferation and cytotoxicity against FHC cells

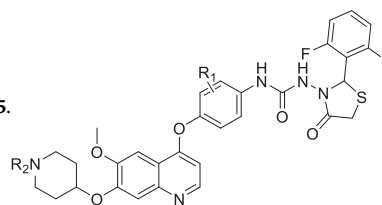
Cell selectivity was evaluated by determining the kinetics of antiproliferation and cytotoxicity against FHC cells. To our delight, compound **15i** exhibited fairly lower toxic to FHC cells than that of Regorafenib. As shown in Figs. 7A and 8, compound **15i** (10.0 µg/mL) displayed over 3-fold shift in the number of dead cells compared to Regorafenib. After treatment with 10.0 µg/mL of compound **15i** for 72 h, the cell confluence reached to 36.5% which was almost equipotent to that of 0.1% DMSO (39.9%). At the same concentration, Regorafenib could significantly inhibit cell proliferation after 72 h (13.5%). Moreover, antiproliferation of compound **15i** against FHC cells was not significant at lower concentration (data not shown).

3.3.3. Measurement of apoptosis

In order to investigate whether the *in vitro* antitumor activity of compound **15i** was caused by the activation of cellular apoptosis. HT-29 cells were stimulated with 0.3–3.0 µg/mL concentrations of compound **15i** for 72 h. As indicated in Figs. 9 and 10, no significant inducing apoptosis was observed during the first 36 h. Exhilaratingly, the apoptosis induced by compound **15i** was much greater than that of

Table 1

In vitro kinase inhibitory activity and anticancer activity of compounds 15a-j and 25.



Compd.	R ₁	R ₂	Inhibitory rate (%) ^a		HT-29 IC ₅₀ (μM) ^b
			c-Met	Ron	
15a	H		18.7	32.3	1.48 ± 0.12
15b	H		19.3	34.7	1.57 ± 0.13
15c	H		37.9	45.1	0.61 ± 0.043
15d	H		37.1	30.8	0.76 ± 0.072
15e	H		16.9	22.6	1.64 ± 0.13
15f	H		17.5	24.4	1.81 ± 0.16
15g	H		29.0	19.8	1.24 ± 0.11
15h	H		16.7	11.5	1.97 ± 0.17
15i	2-F		76.3	89.3	0.19 ± 0.012
15j	3-F		66.7	72.4	0.43 ± 0.031
25			9.7	7.0	–
Regorafenib	–	–	ND ^c	ND	2.75 ± 0.18

^a The kinase inhibition rates at 1.0 μM (c-Met) and 0.5 μM (Ron) are the average of two independent experiments.

^b The values were an average of three separate determinations and standard deviations were shown.

^c ND: Not determined.

Regorafenib after treatment for 36 h.

3.4. Effects on cell cycle progression

In order to investigate the mechanism of antitumor activity and inducing apoptosis, flow cytometry analysis in HT-29 cells treated with compound **15i** and Regorafenib was performed. As shown in Fig. 11, compound **15i** strongly arrested cell cycle progression in the G2/M phase in a dose-dependent manner. The percentage of G2/M cells increased from 12.48% to 57.55% after treatment with compound **15i** at 0.3 μg/mL, 1.0 μg/mL and 3.0 μg/mL.

3.5. *In vitro* kinase profile

In order to investigate potential targets preliminarily, inhibitory activity of the most potent compound **15i** toward tyrosine kinases was assessed by screening against 8 kinases including c-Src, PDGFRα, c-Met, Ron, AXL, B-Raf, c-Kit and IGF1R. As can be seen in Table 2, compound **15i** potently inhibited the kinase activity of Ron with an IC₅₀ value of 0.092 μM. Moreover, it also showed potential inhibitory activity against

c-Src, PDGFRα, c-Met and AXL. The above results suggested that compound **15i** was a potent multi-kinase inhibitor, other targets will be investigated after further structural modification.

4. Conclusions

Based on our previous study, a novel series of quinoline analogues bearing thiazolidinones were designed, synthesized and evaluated for their biological activities. Structure activity relationship analysis was performed based on the results of biological evaluation and docking study. The most promising compound **15i** could inhibit the activity of Ron, c-Met and c-Src, etc. The results of IncuCyte live-cell imaging assays showed that compound **15i** performed excellent cytotoxicity, anti-proliferation and induction of apoptosis on HT-29 cells in a time- and dose-dependent manner with an efficacy that was significantly greater than Regorafenib. The results of flow cytometry indicated that compound **15i** could induce considerable cell cycle arrest in the G2/M stage in HT-29 cells. In addition, no antiproliferation and cytotoxicity against human normal colorectal mucosa epithelial cell FHC was observed at 10.0 μg/mL which indicated that the toxicity to normal cells of

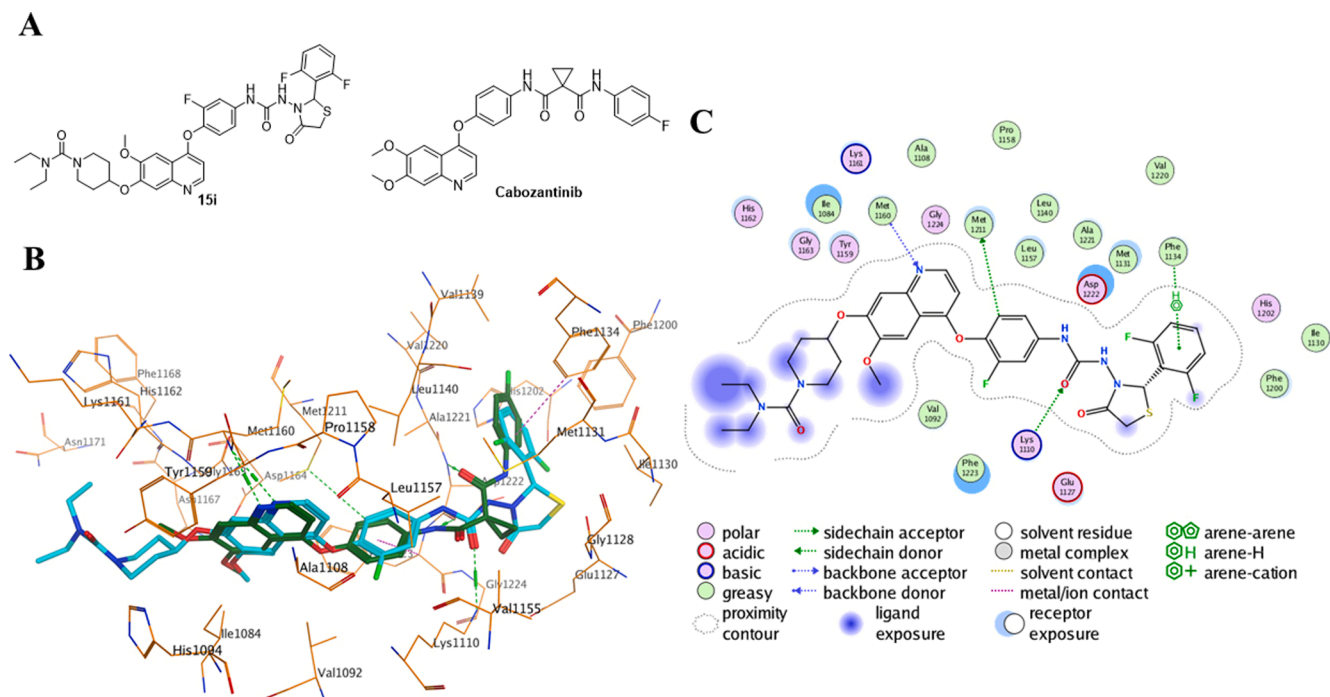


Fig. 3. Binding modes of compound **15i** and Cabozantinib with c-Met kinase (PBD ID: 3LQ8). A) The structures of compound **15i** and Cabozantinib. B) The interactions of compound **15i** and Cabozantinib with c-Met. Compound **15i** and Cabozantinib was shown by blue and dark green sticks, respectively. The H-bonds were represented by green dotted lines, and the H-arene interaction was shown by purple dotted lines. C) 2D depiction of the ligand-protein interactions. (For interpretation of the references to colour in this figure legend, the reader is referred to the web version of this article.)

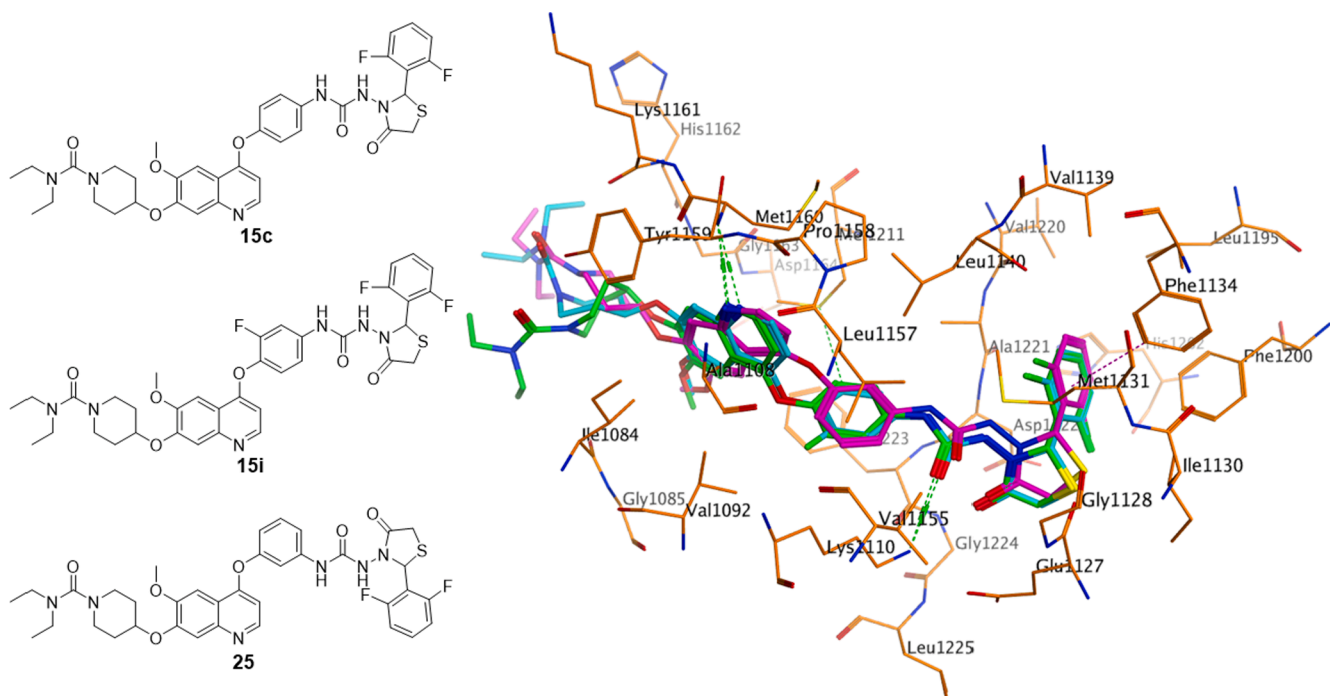


Fig. 4. The superposition of compounds **15c**, **15i** and **25**. The compounds **15c**, **15i** and **25** were shown by green, blue and purple sticks, respectively. The H-bonds were represented by green dotted lines and the H-arene interaction was shown by purple dotted lines. (For interpretation of the references to colour in this figure legend, the reader is referred to the web version of this article.)

compound **15i** was much lower than that of Regorafenib. With the aim of further structural optimization to improve its inhibitory activity in the future, this series of compounds might serve as a good basis for the development of more potent kinase inhibitors as anticancer agents.

5. Experimental

5.1. Chemistry

Commercially available starting materials, reagents, and dry solvents

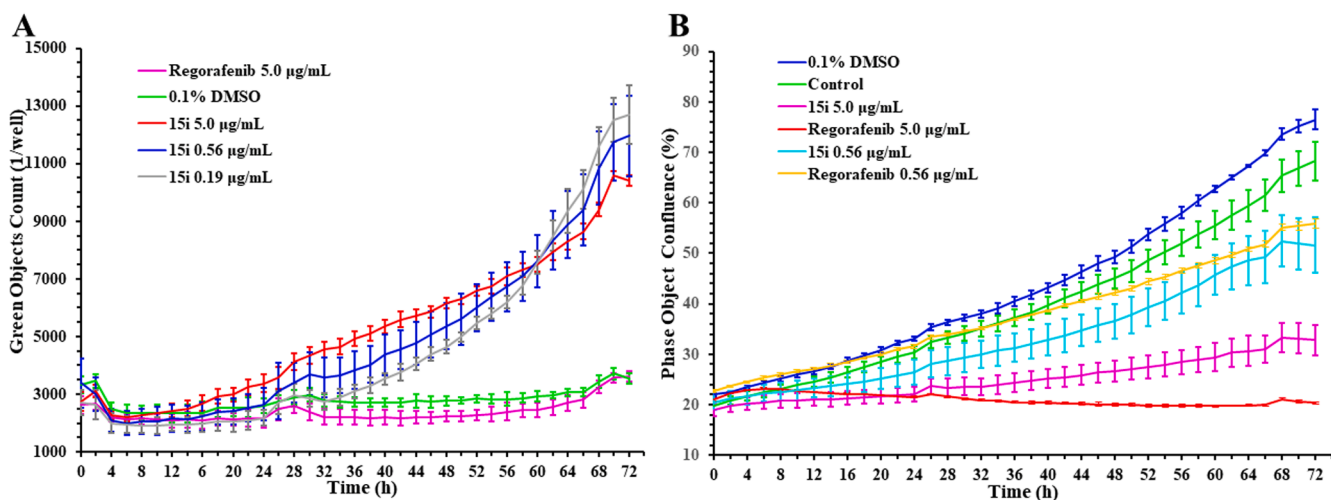


Fig. 5. The antiproliferative and cytotoxic curves of compound 15i on HT-29 cells. All error bars are expressed as mean \pm SD of three independent experiments. A) The curves of real-time cytotoxicity. The number of dead cells was monitored for 72 h using an IncuCyte ZOOM system in an incubator. B) The curves of real-time cell confluence. The cell population was monitored for 72 h using an IncuCyte ZOOM system in an incubator.

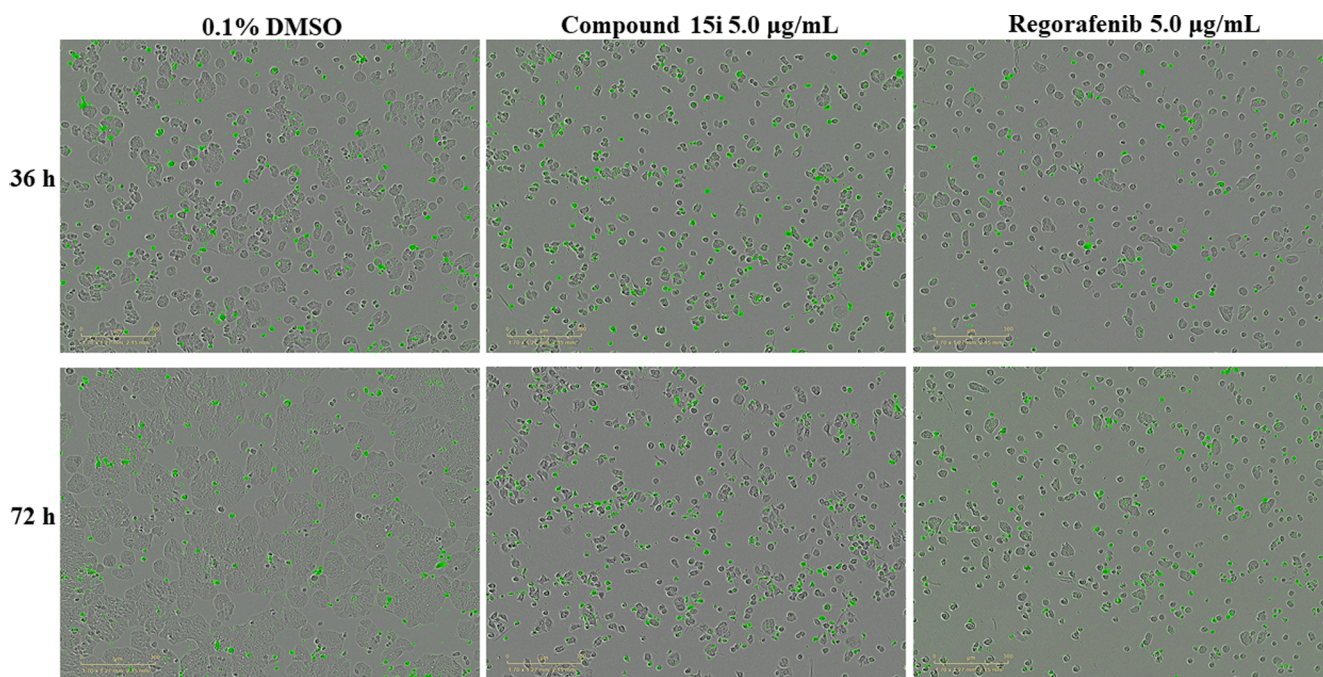


Fig. 6. The white light images (merged) of study on antiproliferation and cytotoxicity against HT-29 cells after 36 h and 72 h of treatment with 0.1% DMSO, compound 15i, or Regorafenib. Green fluorescent cells were counted as dead cell. Nucleus were stained with the DNA fluorescent probe YOYO-1 iodide. (For interpretation of the references to colour in this figure legend, the reader is referred to the web version of this article.)

were used as supplied. ^1H NMR and ^{13}C NMR was generated on Bruker ARX-400 spectrometers (Bruker Bioscience, Billerica, MA, USA). Chemical shifts are given in parts per million (ppm) relative to TMS as internal standards. Column chromatography was performed using Haiyangchem (Qingdao, China) silica gel (200–300 mesh). High Resolution Mass spectra (HRMS) were performed on Agilent 6530 Q-TOF (Agilent Technologies, CA, USA) with ESI source.

5.1.1. General procedure for the synthesis of intermediates 6a-c

To a mixture of 7-(benzyloxy)-4-chloro-6-methoxyquinoline (30.0 g, 0.1 mol) in dry PhCl (180 mL) was added nitrophenols (0.15 mol). The reaction mixture was refluxed for 16 h, allowed to cool to room temperature, and concentrated under vacuum. The residue was treated with CH_2Cl_2 (500 mL), washed with 10% NaOH aqueous solution (3×50 mL)

and water (50 mL) subsequently. The organic layers were dried over Na_2SO_4 and concentrated give the crude products which were used for the next step without further purification.

5.1.1.1. 7-(benzyloxy)-6-methoxy-4-(4-nitrophenoxy)quinoline (6a). Tawny solid, yield: 65.7%. HRMS (ESI) m/z 403.1345 $[\text{M}+\text{H}]^+$, Calcd. for 403.1294.

5.1.1.2. 7-(benzyloxy)-4-(2-fluoro-4-nitrophenoxy)-6-methoxyquinoline (6b). Brown solid, yield: 69.1%. HRMS (ESI) m/z 421.1246 $[\text{M}+\text{H}]^+$, Calcd. for 421.1200.

5.1.1.3. 7-(benzyloxy)-4-(3-fluoro-4-nitrophenoxy)-6-methoxyquinoline (6c). Brown solid, yield: 67.5%. HRMS (ESI) m/z 421.1246 $[\text{M}+\text{H}]^+$,

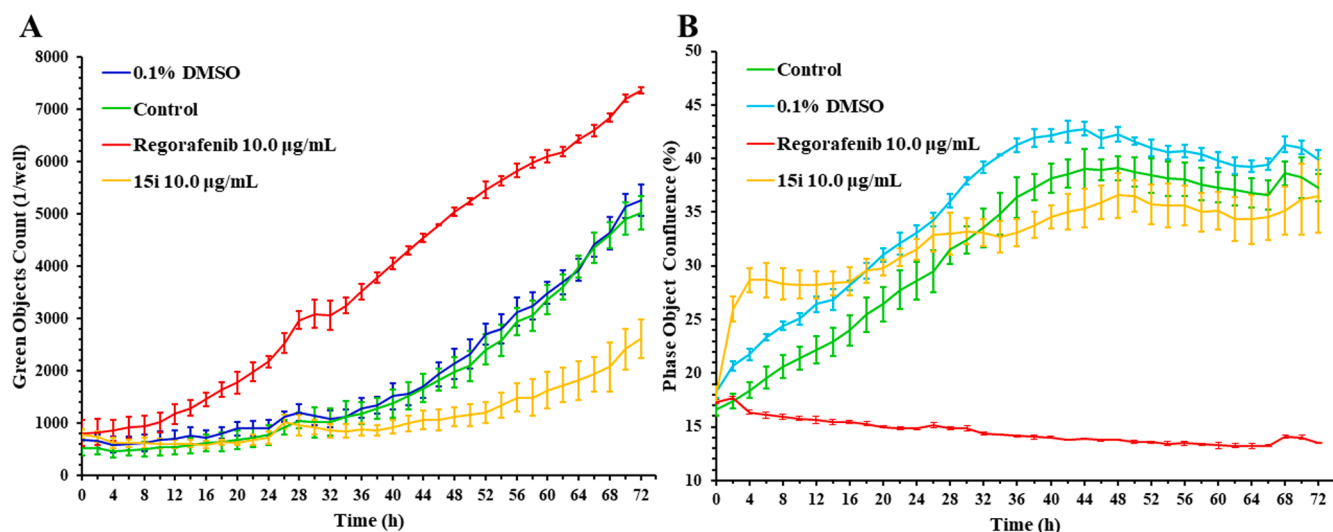


Fig. 7. The antiproliferative and cytotoxic curves of compound **15i** on FHC cells. All error bars are expressed as mean \pm SD of three independent experiments. A) The curves of real-time cytotoxicity. The number of dead cells was monitored for 72 h using an IncuCyte ZOOM system in an incubator. B) The curves of real-time cell confluence. The cell population was monitored for 72 h using an IncuCyte ZOOM system in an incubator.

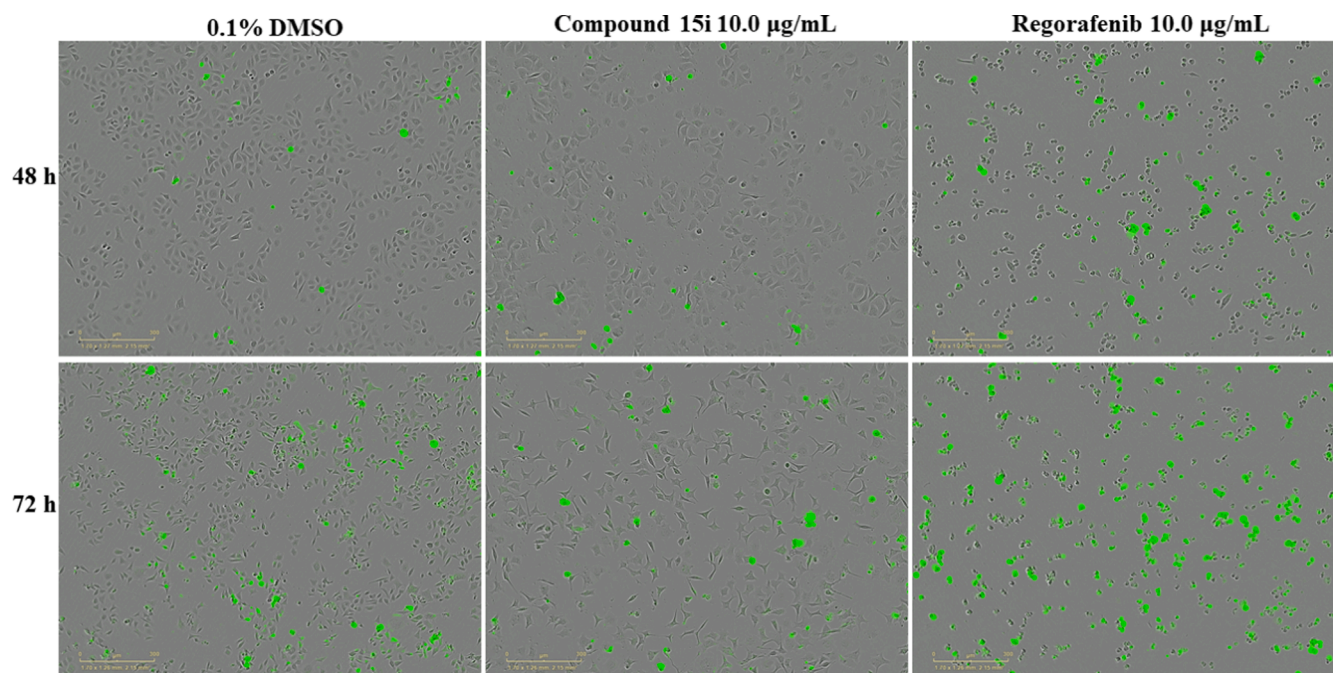


Fig. 8. The white light images (merged) of study on antiproliferation and cytotoxicity against FHC cells after 48 h and 72 h of treatment with compound **15i** (10.0 µg/mL), Regorafenib (10.0 µg/mL) or 0.1% DMSO. Green fluorescent cells were counted as dead cell. Nucleus were stained with the DNA fluorescent probe YOYO-1 iodide. (For interpretation of the references to colour in this figure legend, the reader is referred to the web version of this article.)

Calcd. for 421.1200.

5.1.2. General procedure for the synthesis of intermediates **7a-c**

Intermediates **6a-c** (0.05 mol) was dissolved in 33% HBr in acetic acid (100 mL) and the mixtures were stirred for 3 h at room temperature. The mixture was filtrated, and the solid was washed with isopropyl ether to afford target products.

5.1.2.1. 6-methoxy-4-(4-nitrophenoxy)quinolin-7-ol (7a). Light solid, yield: 66.4%. HRMS (ESI) m/z 313.0872 [M+H]⁺, Calcd. for 313.0824.

5.1.2.2. 4-(2-fluoro-4-nitrophenoxy)-6-methoxyquinolin-7-ol (7b). Yellow solid, yield: 64.2%. HRMS (ESI) m/z 331.0766 [M+H]⁺, Calcd. for

331.0730.

5.1.2.3. 4-(3-fluoro-4-nitrophenoxy)-6-methoxyquinolin-7-ol (7c). Yellow solid, yield: 64.2%. HRMS (ESI) m/z 331.0766 [M+H]⁺, Calcd. for 331.0730.

5.1.3. General procedure for the synthesis of intermediates **8a-c**

To a suspension of intermediates **7a-c** (0.08 mol) and Cs₂CO₃ (0.20 mol) in DMF (100 mL) which was stirred vigorously at room temperature for 10 min, 1-Boc-4-methanesulfonyloxypiperidine (0.12 mol) was added and the mixture was allowed warm to 110 °C for 6 h. The reaction mixture was cooled to room temperature and poured into ice water (400 mL), filtered, and washed with water to give crude **8a-c** which were

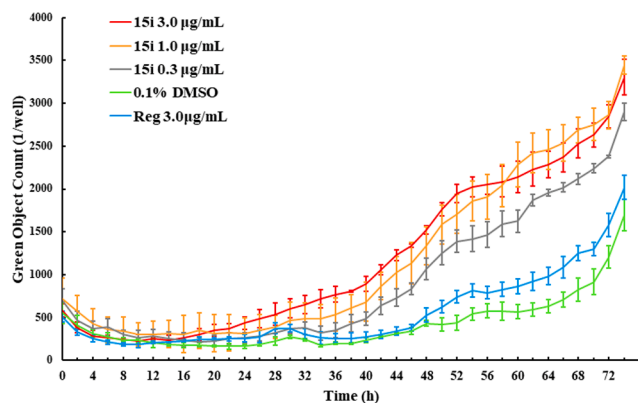


Fig. 9. The apoptosis curves of IncuCyte live-cell imaging assays in HT-29 cells. All error bars are expressed as mean \pm SD of three independent experiments. The cell population was monitored for 72 h using an IncuCyte ZOOM system in an incubator.

purified by column chromatography (eluent, CH_2Cl_2 :MeOH = 100:1 to 15:1) to afford **8a-c**.

5.1.3.1. tert-butyl 4-((6-methoxy-4-(4-nitrophenoxy)quinolin-7-yl)oxy)piperidine-1-carboxylate (8a). Yellow solid, yield: 54.0%. HRMS (ESI) m/z 496.2166 $[\text{M}+\text{H}]^+$, Calcd. for 496.2084.

5.1.3.2. tert-butyl 4-((4-(2-fluoro-4-nitrophenoxy)-6-methoxyquinolin-7-yl)oxy)piperidine-1-carboxylate (8b). Yellow solid, yield: 55.7%. HRMS (ESI) m/z 514.2038 $[\text{M}+\text{H}]^+$, Calcd. for 514.1990.

5.1.3.3. tert-butyl 4-((4-(3-fluoro-4-nitrophenoxy)-6-methoxyquinolin-7-yl)oxy)piperidine-1-carboxylate (8c). Yellow solid, yield: 52.4%. HRMS (ESI) m/z 514.2038 $[\text{M}+\text{H}]^+$, Calcd. for 514.1990.

5.1.4. General procedure for the synthesis of intermediates **9a-c**

To a solution of intermediates **8a-c** (0.05 mol) in CH_2Cl_2 (80 mL),

CF_3COOH (35 mL) was added. The reaction mixture was stirred for 2 h at room temperature and concentrated under vacuum. The residue was dissolved in CH_2Cl_2 (200 mL) and saturated NaHCO_3 aqueous solution was added until the pH reached to 8–9. The organics were dried over Na_2SO_4 , concentrated in vacuo, and the residue was used for the next step without further purification.

5.1.4.1. 6-methoxy-4-(4-nitrophenoxy)-7-(piperidin-4-yloxy)quinoline (9a). Dark yellow oil, yield: 82.4%. ^1H NMR (400 MHz, $\text{DMSO}-d_6$) δ : 8.45 (d, $J = 5.2$ Hz, 1H), 7.92 (m, 2H), 7.49 (s, 1H), 7.15 (m, 3H), 6.46 (d, $J = 5.2$ Hz, 1H), 3.93 (s, 3H), 3.65–3.71 (m, 1H), 3.09–3.16 (m, 4H), 1.98–2.01 (m, 2H), 1.67–1.73 (m, 2H); HRMS (ESI) m/z 396.1621 $[\text{M}+\text{H}]^+$, Calcd. for 396.1559.

5.1.4.2. 4-(2-fluoro-4-nitrophenoxy)-6-methoxy-7-(piperidin-4-yloxy)quinoline (9b). Dark yellow oil, yield: 80.8%. HRMS (ESI) m/z 414.1511 $[\text{M}+\text{H}]^+$, Calcd. for 414.1465.

5.1.4.3. 4-(3-fluoro-4-nitrophenoxy)-6-methoxy-7-(piperidin-4-yloxy)quinoline (9c). Dark yellow oil, yield: 79.2%. HRMS (ESI) m/z 414.1511 $[\text{M}+\text{H}]^+$, Calcd. for 414.1465.

5.1.5. General procedure for the synthesis of intermediates **10a-j**

Acyl chlorides or sulfonyl chlorides (12.0 mmol) was added dropwise to a cold solution of **9a-c** (10.0 mmol) and Et_3N (15.0 mmol) in dry CH_2Cl_2 (50 mL) at 0 $^\circ\text{C}$. After reaction at room temperature for 4–5 h, saturated NaHCO_3 aqueous solution (10 mL) was added, and the organics was separated, dried over Na_2SO_4 , and concentrated in vacuo to afford **10a-j**.

5.1.5.1. furan-2-yl(4-((6-methoxy-4-(4-nitrophenoxy)quinolin-7-yl)oxy)piperidin-1-yl)methanone (10a). Yellow solid, yield: 76.8%. HRMS (ESI) m/z 490.1703 $[\text{M}+\text{H}]^+$, Calcd. for 490.1641.

5.1.5.2. 1-(4-((6-methoxy-4-(4-nitrophenoxy)quinolin-7-yl)oxy)piperidin-1-yl)-2,2-dimethylpropan-1-one (10b). Yellow solid, yield: 81.4%. HRMS (ESI) m/z 480.2177 $[\text{M}+\text{H}]^+$, Calcd. for 480.2135.

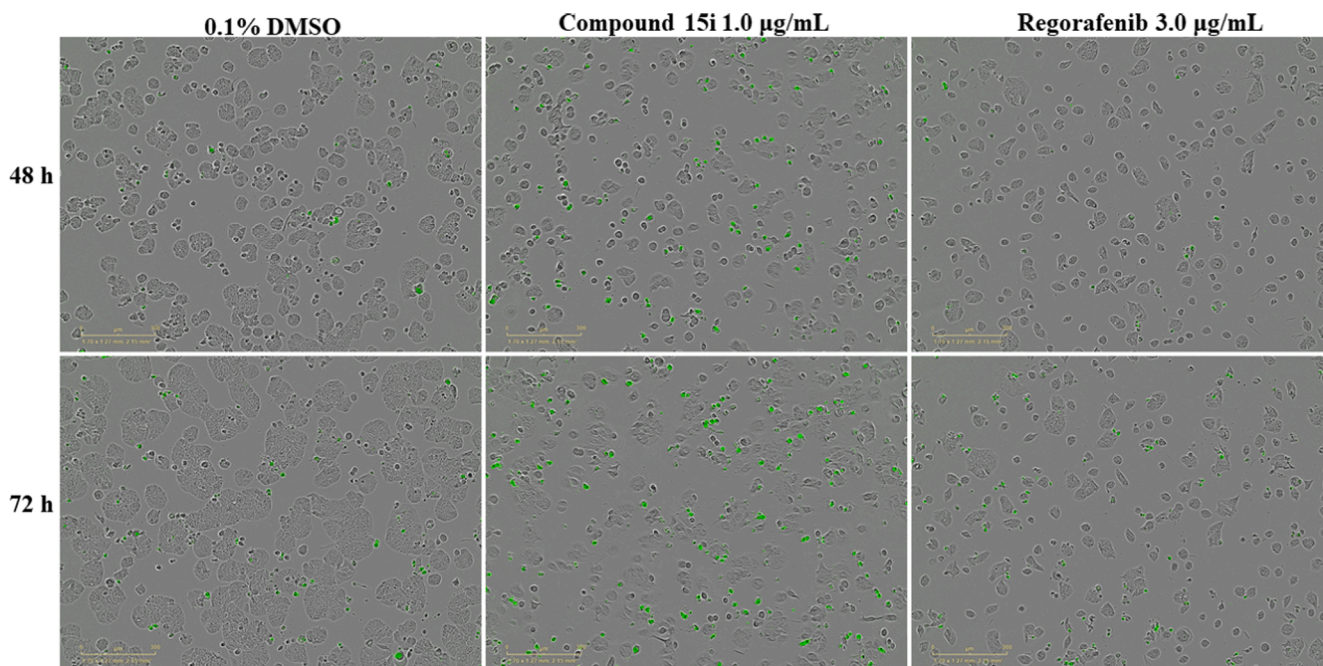


Fig. 10. The white light merged images of study on apoptosis on HT-29 cells after 48 h and 72 h of treatment with 0.1% DMSO, compound **15i** and Regorafenib. Green fluorescent cells were counted as apoptotic cells. Nucleus were stained with the CellEvent™ Caspase 3/7 Green ReadyProbes™ reagent. (For interpretation of the references to colour in this figure legend, the reader is referred to the web version of this article.)

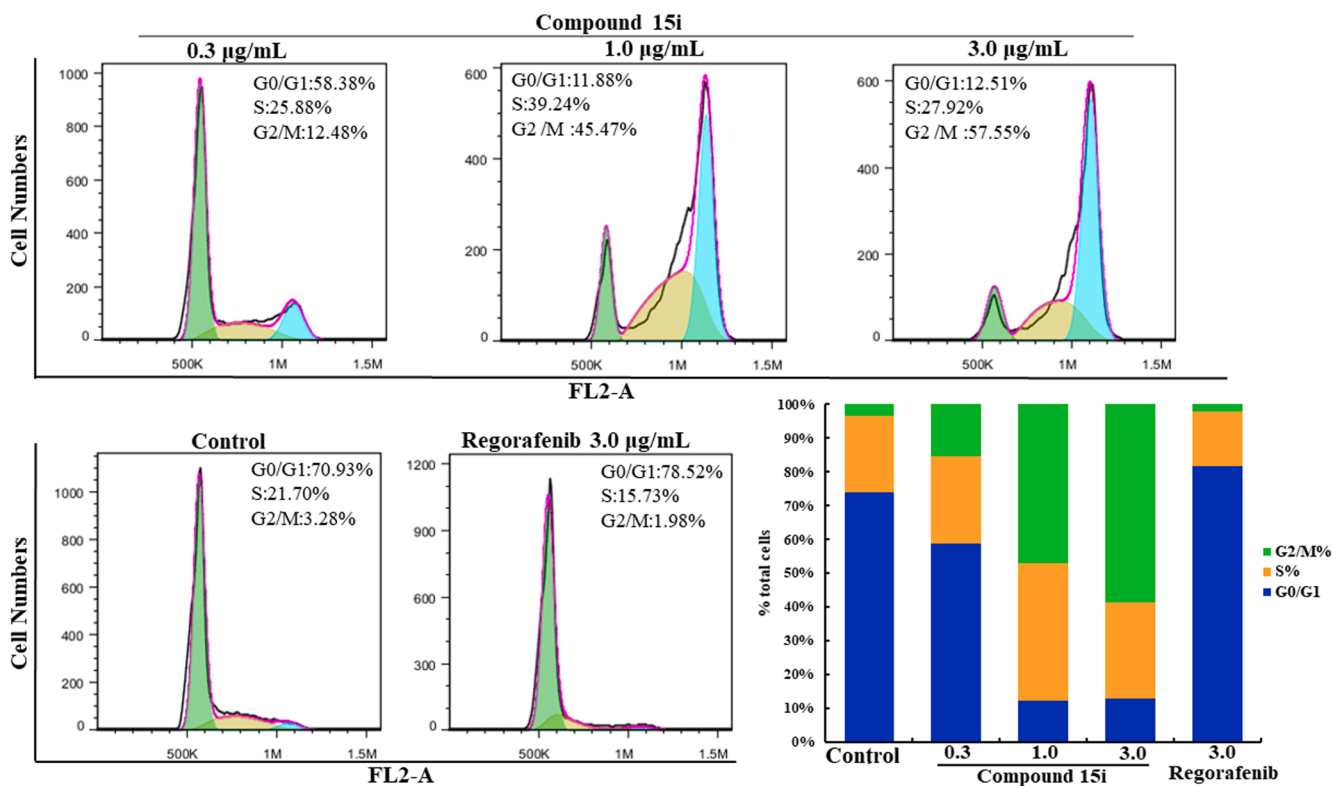


Fig. 11. Cell cycle progression analyses of HT-29 cells treated with compound **15i** (0.3 µg/mL, 1.0 µg/mL and 3.0 µg/mL) and Regorafenib (3.0 µg/mL) for 48 h.

Table 2

The kinase profile of compound **15i**.

Kinases	IC ₅₀ (µM) ^a	Kinases	IC ₅₀ (µM) ^a
c-Met	0.202	PDGFRα	0.212
Ron	0.092	c-Src	0.321
c-Kit	>10.0	IGF1R	>10.0
AXL	0.332	B-Raf	>10.0

^a Values are expressed as the mean of two independent experiments.

5.1.5.3. *N,N*-diethyl-4-((6-methoxy-4-(4-nitrophenoxy)quinolin-7-yl)oxy)piperidine-1-carboxamide (**10c**). Yellow solid, yield: 78.8%. HRMS (ESI) *m/z* 495.2278 [M+H]⁺, Calcd. for 495.2244.

5.1.5.4. 4-((6-methoxy-4-(4-nitrophenoxy)quinolin-7-yl)oxy)-*N,N*-dimethylpiperidine-1-carboxamide (**10d**). Yellow solid, yield: 74.7%. HRMS (ESI) *m/z* 467.1967 [M+H]⁺, Calcd. for 467.1931.

5.1.5.5. 4-((6-methoxy-4-(4-nitrophenoxy)quinolin-7-yl)oxy)-*N,N*-dimethylpiperidine-1-sulfonamide (**10e**). Yellow solid, yield: 82.5%. HRMS (ESI) *m/z* 503.1642 [M+H]⁺, Calcd. for 503.1600.

5.1.5.6. 4-((4-((6-methoxy-4-(4-nitrophenoxy)quinolin-7-yl)oxy)piperidin-1-yl)sulfonyl)morpholine (**10f**). Yellow solid, yield: 73.9%. HRMS (ESI) *m/z* 545.1754 [M+H]⁺, Calcd. for 545.1706.

5.1.5.7. 7-((1-(ethylsulfonyl)piperidin-4-yl)oxy)-6-methoxy-4-(4-nitrophenoxy)quinoline (**10g**). Yellow solid, yield: 78.6%. HRMS (ESI) *m/z* 488.1533 [M+H]⁺, Calcd. for 488.1491.

5.1.5.8. 6-methoxy-4-(4-nitrophenoxy)-7-((1-(thiophen-2-ylsulfonyl)piperidin-4-yl)oxy)quinoline (**10h**). Yellow solid, yield: 77.8%. HRMS (ESI) *m/z* 542.1083 [M+H]⁺, Calcd. for 542.1056.

5.1.5.9. *N,N*-diethyl-4-((4-(2-fluoro-4-nitrophenoxy)-6-methoxyquinolin-7-yl)oxy)piperidine-1-carboxamide (**10i**). Yellow solid, yield: 72.4%. HRMS (ESI) *m/z* 513.2173 [M+H]⁺, Calcd. for 513.2149.

5.1.5.10. *N,N*-diethyl-4-((4-(3-fluoro-4-nitrophenoxy)-6-methoxyquinolin-7-yl)oxy)piperidine-1-carboxamide (**10j**). Yellow solid, yield: 74.4%. HRMS (ESI) *m/z* 513.2172 [M+H]⁺, Calcd. for 513.2149.

5.1.6. General procedure for the synthesis of intermediates **11a-j**

Powered iron (1.68 g, 30.0 mol) and concentrated HCl (2 drops) was added to a suspension of **6** (10.0 mol) in 90% EtOH (50 mL). The reaction mixture was refluxed for 4–6 h. The hot mixture was filtered through celites and the filtrate was evaporated under vacuum to afford intermediates **11a-j**.

5.1.6.1. 4-((4-(4-aminophenoxy)-6-methoxyquinolin-7-yl)oxy)piperidin-1-yl(furan-2-yl)methanone (**11a**). Yellow solid, yield: 76.6%. HRMS (ESI) *m/z* 460.1904 [M+H]⁺, Calcd. for 460.1872.

5.1.6.2. 1-(4-((4-(4-aminophenoxy)-6-methoxyquinolin-7-yl)oxy)piperidin-1-yl)-2,2-dimethylpropan-1-one (**11b**). Yellow solid, yield: 78.5%. HRMS (ESI) *m/z* 450.2431 [M+H]⁺, Calcd. for 450.2393.

5.1.6.3. 4-((4-(4-aminophenoxy)-6-methoxyquinolin-7-yl)oxy)-*N,N*-diethylpiperidine-1-carboxamide (**11c**). Yellow solid, yield: 81.2%. HRMS (ESI) *m/z* 465.2547 [M+H]⁺, Calcd. for 465.2502.

5.1.6.4. 4-((4-(4-aminophenoxy)-6-methoxyquinolin-7-yl)oxy)-*N,N*-dimethylpiperidine-1-carboxamide (**11d**). Yellow solid, yield: 78.9%. HRMS (ESI) *m/z* 437.2225 [M+H]⁺, Calcd. for 437.2189.

5.1.6.5. 4-((4-(4-aminophenoxy)-6-methoxyquinolin-7-yl)oxy)-*N,N*-dimethylpiperidine-1-sulfonamide (**11e**). Yellow solid, yield: 74.4%. HRMS (ESI) *m/z* 473.1891 [M+H]⁺, Calcd. for 473.1859.

5.1.6.6. 4-((6-methoxy-7-((1-(morpholinylsulfonyl)piperidin-4-yl)oxy)quinolin-4-yl)oxy)aniline (**11f**). Yellow solid, yield: 80.6%. HRMS (ESI) m/z 515.2002 $[M+H]^+$, Calcd. for 515.1964.

5.1.6.7. 4-((7-((1-(ethylsulfonyl)piperidin-4-yl)oxy)-6-methoxyquinolin-4-yl)oxy)aniline (**11g**). Yellow solid, yield: 83.4%. HRMS (ESI) m/z 458.1787 $[M+H]^+$, Calcd. for 458.1750.

5.1.6.8. 4-((6-methoxy-7-((1-(thiophen-2-ylsulfonyl)piperidin-4-yl)oxy)quinolin-4-yl)oxy)aniline (**11h**). Yellow solid, yield: 74.3%. HRMS (ESI) m/z 512.1352 $[M+H]^+$, Calcd. for 512.1314.

5.1.6.9. 4-((4-(4-amino-2-fluorophenoxy)-6-methoxyquinolin-7-yl)oxy)-*N,N*-diethylpiperidine-1-carboxamide (**11i**). Yellow solid, yield: 72.8%. HRMS (ESI) m/z 483.2446 $[M+H]^+$, Calcd. for 483.2408.

5.1.6.10. 4-((4-(4-amino-3-fluorophenoxy)-6-methoxyquinolin-7-yl)oxy)-*N,N*-diethylpiperidine-1-carboxamide (**11j**). Yellow solid, yield: 74.9%. HRMS (ESI) m/z 483.2476 $[M+H]^+$, Calcd. for 483.2408.

5.1.7. General procedure for the synthesis of intermediates **13a-j**

To a solution of intermediates **11a-j** (5.0 mmol) and dry pyridine (20.0 mmol) in dry CH_2Cl_2 (20 mL), phenyl chloroformate (10.0 mmol) was added dropwise at 0 °C. After stirring at room temperature for 2 h, saturated $NaHCO_3$ aqueous solution (2 × 20 mL) was added to the solution. The organics was separated, washed with water (20 mL), dried over anhydrous Na_2SO_4 , concentrated in vacuo at room temperature to yield esters **12a-j**, which were immediately used in the following step without further purification.

Intermediates **12a-j** and hydrazine monohydrate (80%, 7 mL) was added to xylene (10 mL), and the reaction mixture was stirred vigorously at 70 °C for 2 h. After cooling to room temperature, the solvent was concentrated under reduced pressure. The residue was purified by silica gel column chromatography (eluent, CH_2Cl_2 : MeOH: Et_3N = 100:2:1 to 100:10:1) to afford semicarbazides **13a-j**.

5.1.7.1. *N*-4-((7-((1-(furan-2-carbonyl)piperidin-4-yl)oxy)-6-methoxyquinolin-4-yl)oxy)phenyl)hydrazinecarboxamide (**13a**). Yellow solid, yield: 32.7%. HRMS (ESI) m/z 518.2072 $[M+H]^+$, Calcd. for 518.2040.

5.1.7.2. *N*-4-((6-methoxy-7-((1-pivaloylpiperidin-4-yl)oxy)quinolin-4-yl)oxy)phenyl)hydrazinecarboxamide (**13b**). Yellow solid, yield: 35.8%. HRMS (ESI) m/z 508.2602 $[M+H]^+$, Calcd. for 508.2560.

5.1.7.3. *N,N*-diethyl-4-((4-(4-(hydrazinecarboxamido)phenoxy)-6-methoxyquinolin-7-yl)oxy)piperidine-1-carboxamide (**13c**). Yellow solid, yield: 34.2%. HRMS (ESI) m/z 523.2703 $[M+H]^+$, Calcd. for 523.2669.

5.1.7.4. 4-((4-(4-(hydrazinecarboxamido)phenoxy)-6-methoxyquinolin-7-yl)oxy)-*N,N*-dimethylpiperidine-1-carboxamide (**13d**). Yellow solid, yield: 34.9%. HRMS (ESI) m/z 495.2389 $[M+H]^+$, Calcd. for 495.2356.

5.1.7.5. *N*-4-((7-((1-(*N,N*-dimethylsulfamoyl)piperidin-4-yl)oxy)-6-methoxyquinolin-4-yl)oxy)phenyl)hydrazinecarboxamide (**13e**). Yellow solid, yield: 38.9%. HRMS (ESI) m/z 531.2059 $[M+H]^+$, Calcd. for 531.2026.

5.1.7.6. *N*-4-((6-methoxy-7-((1-(morpholinylsulfonyl)piperidin-4-yl)oxy)quinolin-4-yl)oxy)phenyl)hydrazinecarboxamide (**13f**). Yellow solid, yield: 38.0%. HRMS (ESI) m/z 573.2169 $[M+H]^+$, Calcd. for 573.2131.

5.1.7.7. *N*-4-((7-((1-(ethylsulfonyl)piperidin-4-yl)oxy)-6-methoxyquinolin-4-yl)oxy)phenyl)hydrazinecarboxamide (**13g**). Yellow solid, yield: 34.2%. HRMS (ESI) m/z 516.1953 $[M+H]^+$, Calcd. for 516.1917.

5.1.7.8. *N*-4-((6-methoxy-7-((1-(thiophen-2-ylsulfonyl)piperidin-4-yl)oxy)quinolin-4-yl)oxy)phenyl)hydrazinecarboxamide (**13h**). Yellow solid, yield: 39.4%. HRMS (ESI) m/z 570.1519 $[M+H]^+$, Calcd. for 570.1481.

5.1.7.9. *N,N*-diethyl-4-((4-(2-fluoro-4-(hydrazinecarboxamido)phenoxy)-6-methoxyquinolin-7-yl)oxy)piperidine-1-carboxamide (**13i**). Yellow solid, yield: 41.2%. HRMS (ESI) m/z 541.2605 $[M+H]^+$, Calcd. for 541.2575.

5.1.7.10. *N,N*-diethyl-4-((4-(3-fluoro-4-(hydrazinecarboxamido)phenoxy)-6-methoxyquinolin-7-yl)oxy)piperidine-1-carboxamide (**13j**). Yellow solid, yield: 39.4%. HRMS (ESI) m/z 541.2613 $[M+H]^+$, Calcd. for 541.2575.

5.1.8. General procedure for the synthesis of intermediates **14a-j**

To a stirred solution of **13a-j** (2.0 mmol) and 2,6-difluorobenzaldehyde (0.34 g, 2.4 mmol) in dry *i*-PrOH (10 mL), acetic acid (2 drops) were added. After refluxing for 2 h, the mixture was allowed to cooled to 0 °C, and the resultant precipitate was filtered, washed with cold *i*-PrOH and dried in vacuo to afford semicarbazones **14a-j**.

5.1.8.1. (*E*)-2-(2,6-difluorobenzylidene)-*N*-4-((7-((1-(furan-2-carbonyl)piperidin-4-yl)oxy)-6-methoxyquinolin-4-yl)oxy)phenyl)hydrazine-1-carboxamide (**14a**). White solid, yield: 81.2%. HRMS (ESI) m/z 642.2258 $[M+H]^+$, Calcd. for 642.2164.

5.1.8.2. (*E*)-2-(2,6-difluorobenzylidene)-*N*-4-((6-methoxy-7-((1-pivaloylpiperidin-4-yl)oxy)quinolin-4-yl)oxy)phenyl)hydrazine-1-carboxamide (**14b**). White solid, yield: 78.5%. HRMS (ESI) m/z 632.2738 $[M+H]^+$, Calcd. for 632.2685.

5.1.8.3. (*E*)-4-((4-(2-(2,6-difluorobenzylidene)hydrazine-1-carboxamido)phenoxy)-6-methoxyquinolin-7-yl)oxy)-*N,N*-diethylpiperidine-1-carboxamide (**14c**). White solid, yield: 80.4%. HRMS (ESI) m/z 647.2847 $[M+H]^+$, Calcd. for 647.2793.

5.1.8.4. (*E*)-4-((4-(2-(2,6-difluorobenzylidene)hydrazine-1-carboxamido)phenoxy)-6-methoxyquinolin-7-yl)oxy)-*N,N*-dimethylpiperidine-1-carboxamide (**14d**). White solid, yield: 85.0%. HRMS (ESI) m/z 619.2534 $[M+H]^+$, Calcd. for 619.2480.

5.1.8.5. (*E*)-2-(2,6-difluorobenzylidene)-*N*-4-((7-((1-(*N,N*-dimethylsulfamoyl)piperidin-4-yl)oxy)-6-methoxyquinolin-4-yl)oxy)phenyl)hydrazine-1-carboxamide (**14e**). White solid, yield: 82.4%. HRMS (ESI) m/z 655.2206 $[M+H]^+$, Calcd. for 655.2150.

5.1.8.6. (*E*)-2-(2,6-difluorobenzylidene)-*N*-4-((6-methoxy-7-((1-(morpholinylsulfonyl)piperidin-4-yl)oxy)quinolin-4-yl)oxy)phenyl)hydrazine-1-carboxamide (**14f**). White solid, yield: 79.7%. HRMS (ESI) m/z 697.2308 $[M+H]^+$, Calcd. for 697.2256.

5.1.8.7. (*E*)-2-(2,6-difluorobenzylidene)-*N*-4-((7-((1-(ethylsulfonyl)piperidin-4-yl)oxy)-6-methoxyquinolin-4-yl)oxy)phenyl)hydrazine-1-carboxamide (**14g**). White solid, yield: 80.7%. HRMS (ESI) m/z 640.2102 $[M+H]^+$, Calcd. for 640.2041.

5.1.8.8. (*E*)-2-(2,6-difluorobenzylidene)-*N*-4-((6-methoxy-7-((1-(thiophen-2-ylsulfonyl)piperidin-4-yl)oxy)quinolin-4-yl)oxy)phenyl)hydrazine-1-carboxamide (**14h**). White solid, yield: 79.8%. HRMS (ESI) m/z 694.1664 $[M+H]^+$, Calcd. for 694.1606.

5.1.8.9. (*E*)-4-((4-(2-(2,6-difluorobenzylidene)hydrazine-1-carboxamido)-2-fluorophenoxy)-6-methoxyquinolin-7-yl)oxy)-*N,N*-diethylpiperidine-1-carboxamide (**14i**). White solid, yield: 80.6%. HRMS (ESI) m/z

665.2757 [M+H]⁺, Calcd. for 665.2699.

5.1.8.10. (E)-4-((4-(4-(2-(2,6-difluorobenzylidene)hydrazine-1-carboxamido)-3-fluorophenoxy)-6-methoxyquinolin-7-yl)oxy)-N,N-diethylpiperidine-1-carboxamide (**14j**). White solid, yield: 82.4%. HRMS (ESI) *m/z* 665.2757 [M+H]⁺, Calcd. for 665.2699.

5.1.9. General procedure for the synthesis of target compounds **15a-j**

To a solution of semicarbazides **14a-j** (0.5 mmol) and mercaptoacetic acid (0.5 mL) in dry CH₂Cl₂ (10 mL), SiCl₄ (20 drops) were added at room temperature. After the resulting mixture refluxed for 6 h, the reaction mixture was allowed to cooled to room temperature before quenched by ice water, and 10% NaOH aqueous solution was added until pH reached to 9–10. The organic phase was separated and washed with water (2 × 5 mL), concentrated under vacuum to afford yellow oil which was purified by silica gel column chromatography (eluent, CH₂Cl₂: MeOH: Et₃N = 100:5:1 to 100:10:1) to afford target compounds **15a-j**.

5.1.9.1. 1-(2-(2,6-difluorophenyl)-4-oxothiazolidin-3-yl)-3-(4-((7-((1-(furan-2-carbonyl)piperidin-4-yl)oxy)-6-methoxyquinolin-4-yl)oxy)phenyl)urea (**15a**). White solid, yield: 39.1%. ¹H NMR (400 MHz, DMSO-*d*₆) δ: 8.97 (s, 1H), 8.77 (s, 1H), 8.46 (d, *J* = 5.2 Hz, 1H), 7.85 (m, 1H), 7.48–7.55 (m, 5H), 7.16–7.21 (m, 4H), 7.03 (m, 1H), 6.64 (m, 1H), 6.43 (d, *J* = 5.2 Hz, 1H), 6.17 (s, 1H), 4.93–4.97 (m, 1H), 4.02–4.07 (m, 2H), 3.94 (s, 3H), 3.85 (s, 2H), 3.58 (br, 2H), 2.12–2.15 (m, 2H), 1.71–1.78 (m, 2H); ¹³C NMR (100 MHz, DMSO-*d*₆) δ: 169.0, 164.3, 160.6, 154.3, 150.5, 150.4, 149.3, 149.0, 147.2, 146.7, 142.6, 137.1, 132.1, 132.0, 122.0 (2C), 120.6, 117.7, 115.7 (2C), 115.3, 115.2, 112.9, 112.7, 111.5, 110.9, 103.4, 100.1, 73.7, 56.2, 52.3, 44.2 (2C), 30.6 (2C), 29.7. HRMS (ESI) *m/z* 738.1949 [M+Na]⁺, Calcd. for 738.1810.

5.1.9.2. 1-(2-(2,6-difluorophenyl)-4-oxothiazolidin-3-yl)-3-(4-((6-methoxy-7-((1-pivaloylpiperidin-4-yl)oxy)quinolin-4-yl)oxy)phenyl)urea (**15b**). White solid, yield: 45.2%. ¹H NMR (400 MHz, DMSO-*d*₆) δ: 8.97 (s, 1H), 8.77 (s, 1H), 8.46 (d, *J* = 5.2 Hz, 1H), 7.49–7.55 (m, 5H), 7.17–7.21 (m, 4H), 6.41 (d, *J* = 5.2 Hz, 1H), 6.17 (s, 1H), 4.87–4.91 (m, 1H), 4.02–4.07 (m, 2H), 3.94–3.99 (m, 4H), 3.85 (m, 3H), 3.41–3.47 (m, 1H), 3.24–3.29 (m, 1H), 2.00–2.07 (m, 2H), 1.59–1.67 (m, 2H), 1.03 (s, 3H), 1.02 (s, 3H), 0.97 (s, 3H); ¹³C NMR (100 MHz, DMSO-*d*₆) δ: 169.0, 164.3, 160.6, 154.3, 150.5, 150.4, 149.3, 149.0, 146.7, 137.1, 132.1, 132.0, 122.0 (2C), 120.6, 115.7 (2C), 115.3, 115.2, 112.9, 112.7, 110.9, 103.4, 100.1, 73.7, 56.2, 52.3, 44.2 (2C), 38.7, 30.6 (2C), 29.7, 27.5 (3C). HRMS (ESI) *m/z* 728.2395 [M+Na]⁺, Calcd. for 728.2330.

5.1.9.3. 4-((4-(4-(3-(2-(2,6-difluorophenyl)-4-oxothiazolidin-3-yl)ureido)phenoxy)-6-methoxyquinolin-7-yl)oxy)-N,N-diethylpiperidine-1-carboxamide (**15c**). White solid, yield: 42.6%. ¹H NMR (400 MHz, DMSO-*d*₆) δ: 8.96 (s, 1H), 8.76 (s, 1H), 8.45 (d, *J* = 5.2 Hz, 1H), 7.50–7.55 (m, 5H), 7.17–7.21 (m, 4H), 6.41 (d, *J* = 5.2 Hz, 1H), 6.17 (s, 1H), 4.80–4.84 (m, 1H), 3.94 (s, 3H), 3.85 (s, 2H), 3.42–3.46 (m, 2H), 3.13 (q, *J* = 7.2 Hz, 4H), 3.02–3.08 (m, 2H), 2.03–2.07 (m, 2H), 1.64–1.72 (m, 2H), 1.06 (t, *J* = 7.2 Hz, 6H); ¹³C NMR (100 MHz, DMSO-*d*₆) δ: 169.0, 164.0, 160.6, 154.3, 150.5, 150.4, 149.3, 149.0, 146.7, 137.1, 132.1, 131.9, 122.0 (2C), 120.6, 115.7 (2C), 115.4, 115.3, 112.9, 112.7, 110.9, 103.4, 100.1, 73.7, 56.2, 52.3, 44.5 (2C), 41.9 (2C), 30.6 (2C), 29.8, 13.6 (2C). HRMS (ESI) *m/z* 743.2554 [M+Na]⁺, Calcd. for 743.2439.

5.1.9.4. 4-((4-(4-(3-(2-(2,6-difluorophenyl)-4-oxothiazolidin-3-yl)ureido)phenoxy)-6-methoxyquinolin-7-yl)oxy)-N,N-dimethylpiperidine-1-carboxamide (**15d**). White solid, yield: 39.8%. ¹H NMR (400 MHz, DMSO-*d*₆) δ: 9.00 (s, 1H), 8.79 (s, 1H), 8.44 (d, *J* = 5.2 Hz, 1H), 7.48–7.56 (m, 5H), 7.17–7.21 (m, 4H), 6.42 (d, *J* = 5.2 Hz, 1H), 6.19 (s, 1H), 4.79–4.83 (m, 1H), 3.94 (s, 3H), 3.85 (s, 2H), 3.45–3.48 (m, 2H),

3.02–3.08 (m, 2H), 2.76 (s, 6H), 2.04–2.06 (m, 2H), 1.66–1.71 (m, 2H); ¹³C NMR (100 MHz, DMSO-*d*₆) δ: 169.0, 164.3, 160.6, 154.3, 150.5, 150.4, 149.3, 149.0, 146.7, 137.1, 132.1, 132.0, 122.0 (2C), 120.6, 115.7 (2C), 115.3, 115.2, 112.9, 112.7, 110.9, 103.4, 100.1, 73.7, 56.2, 52.3, 44.2 (2C), 38.6 (2C), 30.6 (2C), 29.7. HRMS (ESI) *m/z* 715.2252 [M+Na]⁺, Calcd. for 715.2126.

5.1.9.5. 4-((4-(4-(3-(2-(2,6-difluorophenyl)-4-oxothiazolidin-3-yl)ureido)phenoxy)-6-methoxyquinolin-7-yl)oxy)-N,N-dimethylpiperidine-1-sulfonamide (**15e**). White solid, yield: 41.6%. ¹H NMR (400 MHz, DMSO-*d*₆) δ: 8.99 (s, 1H), 8.79 (s, 1H), 8.45 (d, *J* = 5.2 Hz, 1H), 7.51–7.54 (m, 5H), 7.17–7.21 (m, 4H), 6.41 (d, *J* = 5.2 Hz, 1H), 6.16 (s, 1H), 4.82 (br, 1H), 3.94 (s, 3H), 3.84 (s, 2H), 3.46 (m, 2H), 3.22 (m, 2H), 2.78 (s, 6H), 2.17 (m, 2H), 1.77 (m, 2H); ¹³C NMR (100 MHz, DMSO-*d*₆) δ: 169.0, 164.3, 160.6, 154.3, 150.5, 150.3, 149.4, 149.0, 146.7, 137.1, 132.0, 131.9, 122.0 (2C), 120.6, 115.8 (2C), 115.6, 115.3, 112.9, 112.7, 111.1, 103.4, 100.1, 72.6, 56.3, 52.3, 43.9 (2C), 38.4 (2C), 30.4 (2C), 29.8. HRMS (ESI) *m/z* 751.1925 [M+Na]⁺, Calcd. for 751.1796.

5.1.9.6. 1-(2-(2,6-difluorophenyl)-4-oxothiazolidin-3-yl)-3-(4-((6-methoxy-7-((1-(morpholin-sulfonyl)piperidin-4-yl)oxy)quinolin-4-yl)oxy)phenyl)urea (**15f**). White solid, yield: 42.0%. ¹H NMR (400 MHz, DMSO-*d*₆) δ: 8.96 (s, 1H), 8.75 (s, 1H), 8.45 (d, *J* = 4.0 Hz, 1H), 7.48–7.54 (m, 5H), 7.17–7.20 (m, 4H), 6.42 (d, *J* = 4.0 Hz, 1H), 6.18 (s, 1H), 4.80–4.83 (m, 1H), 3.94 (s, 3H), 3.84 (s, 2H), 3.49–3.51 (m, 2H), 3.21–3.25 (m, 2H), 3.05–3.08 (m, 2H), 2.09 (br, 2H), 1.69–1.79 (m, 4H), 1.23–1.30 (m, 1H), 1.02 (m, 3H); ¹³C NMR (100 MHz, DMSO-*d*₆) δ: 169.0, 160.6, 154.4, 150.5, 150.3, 149.4, 149.0, 146.6, 137.1, 132.0, 131.9, 122.0 (2C), 120.6, 115.9, 115.6, 115.1 (2C), 112.9, 112.7, 111.1, 103.5, 100.2, 72.6, 56.3, 50.4, 43.1 (2C), 30.6 (2C), 29.8, 17.0 (2C), 13.3 (2C). HRMS (ESI) *m/z* 793.2042 [M+Na]⁺, Calcd. for 793.1902.

5.1.9.7. 1-(2-(2,6-difluorophenyl)-4-oxothiazolidin-3-yl)-3-(4-((7-((1-(ethylsulfonyl)piperidin-4-yl)oxy)-6-methoxyquinolin-4-yl)oxy)phenyl)urea (**15g**). ¹H NMR (400 MHz, DMSO-*d*₆) δ: 8.99 (s, 1H), 8.78 (s, 1H), 8.45 (d, *J* = 5.2 Hz, 1H), 7.48–7.55 (m, 5H), 7.14–7.20 (m, 4H), 6.41 (d, *J* = 5.2 Hz, 1H), 6.17 (s, 1H), 4.82 (s, 1H), 3.94 (s, 3H), 3.84 (s, 2H), 3.50–3.52 (m, 2H), 3.21–3.26 (m, 2H), 3.09–3.13 (q, *J* = 7.2 Hz, 2H), 2.09 (br, 2H), 1.75–1.80 (m, 2H), 1.24 (t, *J* = 7.2 Hz, 3H); ¹³C NMR (100 MHz, DMSO-*d*₆) δ: 169.0, 160.8, 154.3, 150.5, 150.3, 149.4, 149.0, 146.7, 137.1, 132.1, 132.0, 131.9, 122.0 (2C), 120.6, 115.9 (2C), 115.6, 115.3, 112.9, 112.8, 111.2, 103.5, 72.6, 56.3, 52.3, 43.6, 43.1 (2C), 30.6 (2C), 29.8, 8.1. HRMS (ESI) *m/z* 736.1833 [M+Na]⁺, Calcd. for 736.1687.

5.1.9.8. 1-(2-(2,6-difluorophenyl)-4-oxothiazolidin-3-yl)-3-(4-((6-methoxy-7-((1-(thiophen-2-ylsulfonyl)piperidin-4-yl)oxy)quinolin-4-yl)oxy)phenyl)urea (**15h**). White solid, yield: 43.5%. ¹H NMR (400 MHz, DMSO-*d*₆) δ: 8.97 (s, 1H), 8.77 (s, 1H), 8.42 (d, *J* = 5.2 Hz, 1H), 8.10 (m, 1H), 7.68 (m, 1H), 7.48–7.51 (m, 5H), 7.33 (m, 1H), 7.13–7.20 (m, 4H), 6.40 (d, *J* = 5.2 Hz, 1H), 6.16 (s, 1H), 4.77 (m, 1H), 3.80–3.84 (m, 5H), 3.28 (m, 2H), 3.01 (m, 2H), 2.10 (m, 2H), 1.82 (m, 2H); ¹³C NMR (100 MHz, DMSO-*d*₆) δ: 169.0, 164.3, 160.6, 154.3, 150.5, 150.3, 149.4, 149.0, 146.7, 137.1, 132.0, 131.9, 127.4 (2C), 126.2, 125.3, 122.0 (2C), 120.6, 115.8 (2C), 115.6, 115.3, 112.9, 112.7, 111.1, 103.4, 100.1, 72.6, 56.3, 52.3, 43.9 (2C), 30.4 (2C), 22.6. HRMS (ESI) *m/z* 790.1399 [M+Na]⁺, Calcd. for 790.1251.

5.1.9.9. 4-((4-(4-(3-(2-(2,6-difluorophenyl)-4-oxothiazolidin-3-yl)ureido)-2-fluorophenoxy)-6-methoxyquinolin-7-yl)oxy)-N,N-diethylpiperidine-1-carboxamide (**15i**). White solid, yield: 38.9%, purity: 98.14%. ¹H NMR (400 MHz, DMSO-*d*₆) δ: 9.20 (s, 1H), 8.96 (s, 1H), 8.44 (d, *J* = 5.2 Hz, 1H), 7.63–7.66 (m, 1H), 7.47–7.52 (m, 2H), 7.35–7.40 (m, 2H), 7.29 (m, 1H), 7.16–7.21 (m, 2H), 6.41 (d, *J* = 5.2 Hz, 1H), 6.15 (s, 1H), 4.04 (m, 1H), 3.93 (s, 3H), 3.85 (s, 2H), 3.43–3.46 (m, 2H), 3.10 (m, 4H),

2.74 (m, 2H), 1.84 (m, 2H), 1.23–1.28 (m, 2H), 1.05 (t, $J = 7.2$ Hz, 6H); ^{13}C NMR (100 MHz, DMSO- d_6) δ : 169.0, 164.0, 160.6, 154.3, 150.5, 150.4, 149.3, 149.0, 146.7, 137.1, 132.1, 131.9, 122.0 (2C), 120.6, 115.7 (2C), 115.4, 115.2, 112.9, 112.7, 110.8, 103.4, 100.1, 73.7, 56.2, 52.3, 44.5 (2C), 41.9 (2C), 30.6 (2C), 29.8, 13.6 (2C). HRMS (ESI) m/z 761.2359 [M+Na] $^+$, Calcd. for 761.2345.

5.1.9.10. 4-((4-(4-(3-(2-(2,6-difluorophenyl)-4-oxothiazolidin-3-yl)ureido)-3-fluorophenoxy)-6-methoxyquinolin-7-yl)oxy)-N,N-diethylpiperidine-1-carboxamide (15j). White solid, yield: 38.9%. ^1H NMR (400 MHz, DMSO- d_6) δ : 8.98 (s, 1H), 8.78 (s, 1H), 8.44 (d, $J = 5.2$ Hz, 1H), 7.56 (s, 1H), 7.50–7.54 (m, 3H), 7.16–7.20 (m, 4H), 6.41 (d, $J = 5.2$ Hz, 1H), 6.16 (s, 1H), 4.63–4.68 (m, 1H), 3.91 (s, 3H), 3.84 (s, 2H), 3.60–3.63 (m, 2H), 3.02–3.17 (m, 6H), 2.06–2.09 (m, 1H), 1.75–1.78 (m, 2H), 1.53–1.61 (m, 1H), 1.06 (t, $J = 7.2$ Hz, 6H); ^{13}C NMR (100 MHz, DMSO- d_6) δ : 169.0, 164.0, 160.8, 154.3, 150.5, 150.4, 149.3, 149.0, 146.7, 137.1, 132.1, 131.9, 122.0 (2C), 115.7 (2C), 115.4, 115.2, 112.9, 112.7, 110.8, 103.4, 100.1, 73.7, 56.2, 52.3, 43.9 (2C), 41.7 (2C), 30.6 (2C), 29.6, 13.6 (2C). HRMS (ESI) m/z 761.2360 [M+Na] $^+$, Calcd. for 761.2345.

5.1.10. 4-((4-(3-(3-(2-(2,6-difluorophenyl)-4-oxothiazolidin-3-yl)ureido)phenoxy)-6-methoxyquinolin-7-yl)oxy)-N,N-diethylpiperidine-1-carboxamide (25)

White solid, yield: 42.9%. ^1H NMR (400 MHz, DMSO- d_6) δ : 9.05 (s, 1H), 8.81 (s, 1H), 8.48 (d, $J = 5.2$ Hz, 1H), 7.48–7.53 (m, 4H), 7.36–7.41 (m, 2H), 7.25–7.27 (m, 1H), 7.14–7.17 (m, 2H), 6.42 (d, $J = 5.2$ Hz, 1H), 6.17 (s, 1H), 4.80–4.84 (m, 1H), 3.94 (s, 3H), 3.86 (s, 2H), 3.42–3.46 (m, 2H), 3.14 (q, $J = 7.2$ Hz, 4H), 3.02–3.08 (m, 2H), 2.02–2.07 (m, 2H), 1.64–1.71 (m, 2H), 1.06 (t, $J = 7.2$ Hz, 6H); ^{13}C NMR (100 MHz, DMSO- d_6) δ : 169.1, 164.1, 160.7, 154.4, 150.5, 150.2, 149.3, 149.0, 146.7, 137.1, 132.1, 131.9, 122.0 (2C), 120.7, 115.7 (2C), 115.3, 115.2, 112.9, 112.7, 110.8, 103.5, 100.2, 73.8, 56.4, 52.4, 44.6 (2C), 41.9 (2C), 30.8 (2C), 29.9, 13.7 (2C). HRMS (ESI) m/z 743.2588 [M+Na] $^+$, Calcd. for 743.2439.

5.2. MTT assay

The *in vitro* antitumor activity of target compounds were evaluated with human colon cancer cell HT-29 (China Infrastructure of Cell Line Resource) by MTT assay, with Cabozantinib and Regorafenib as positive control. Detailed operation could be found in our previous research [27].

5.3. Mobility shift assay of tyrosine kinases *in vitro*

Kinase inhibitory activity against c-Met, Ron, c-Kit, PDGFR α , BRAF, IGF-1R, c-Src and AXL was evaluated by the mobility shift assay. Detailed operation could be found in our previous research [27].

5.4. IncuCyte live-cell imaging assays

A total of 5×10^3 HT-29 cells (China Infrastructure of Cell Line Resource) and FHC cells (Beijing Beina Chuanglian Biotechnology Institute) grown in 100 μL Dulbecco's Modified Eagle Media (DMEM) with serum (10% FBS) were seeded in 96-well plates respectively and incubated in a tissue culture incubator at 37 $^\circ\text{C}$ and 5% CO_2 in a Live-Cell Imaging Analysis System (Essen BioScience). The cells were cultured for 24 h, and different concentration of compound 15i and Regorafenib were added. Confluency was measured by averaging the percentage of area that the cells occupied from three images of a given well every two hours for 72 h. Assay was performed according to the manufacturer's protocol. To analyze the cytotoxicity, the DNA fluorescent probe YOYO-1 iodide in a solution of DMSO was added. For apoptosis study, the CellEventTM Caspase 3/7 Green ReadyProbesTM

reagent (Thermo Fisher Scientific; R37111) was added. Green fluorescent signals were measured, and green-fluorescent cells were counted as dead cells and apoptotic cells, respectively. All samples consisted of three replicates.

5.5. Cell-cycle assay

HT-29 cells were treated with 0.1% DMSO, compound 15i and Regorafenib at gradient increase from 0.3 to 3.0 $\mu\text{g}/\text{mL}$ for 48 h. Cells were washed with PBS for twice, fixed with 70% cold ethanol at 4 $^\circ\text{C}$ overnight. The cells were stained with propidium iodide for 30 min at room temperature in the dark. Cell-cycle analyses were made with a BD Accuri C6 (Becton Dickinson, Franklin Lakes, NJ, USA) and the data was analyzed using FlowJo7.6.1 Software.

5.6. Molecular docking study

All preparation and docking study were performed with Molecular Operating Environment 2018.01 (MOE, Chemical Computing Group ULC, Montreal, QC, Canada) using default settings. The c-Met receptor structure was prepared (protonation, modeling of missing elements) from the original PDB files (PDB ID: 3LQ8) using Quickprepare, and the strength of receptor was 5000. The binding site was defined within 5.0 Å of the cocrystallized ligands coordinates. The docking forcefield was Amber10: EHT. Ligand conformations were placed in the site with the Triangle Matcher method and ranked using the London dG scoring function.

Declaration of Competing Interest

The authors declare that they have no known competing financial interests or personal relationships that could have appeared to influence the work reported in this paper.

Acknowledgements

This work was supported by the National Natural Science Foundation of China (No. 81960627).

Appendix A. Supplementary data

Supplementary data to this article can be found online at <https://doi.org/10.1016/j.bioorg.2020.104511>.

References

- [1] Z. Knight, H. Lin, K. Shokat, Targeting the cancer kinome through polypharmacology, *Nat. Rev. Cancer* 10 (2010) 130–137, <https://doi.org/10.1038/nrc2787>.
- [2] J.G. Christensen, J. Burrows, R. Salgia, c-Met as a target for human cancer and characterization of inhibitors for therapeutic intervention, *Cancer Lett.* 225 (2005) 1–26, <https://doi.org/10.1016/j.canlet.2004.09.044>.
- [3] C. Birchmeier, W. Birchmeier, E. Gherardi, et al., Met, metastasis, motility and more, *Nat. Rev. Mol. Cell Biol.* 4 (2003) 915–925, <https://doi.org/10.1038/nrm1261>.
- [4] L. Marano, R. Chiari, A. Fabozzi, et al., c-Met targeting in advanced gastric cancer: an open challenge, *Cancer Lett.* 365 (2015) 30–36, <https://doi.org/10.1016/j.canlet.2015.05.028>.
- [5] X. Liu, W. Yao, R.C. Newton, et al., Targeting the c-MET signaling pathway for cancer therapy, *Expert Opin. Investig. Drugs* 17 (2008) 997–1011, <https://doi.org/10.1517/13543784.17.7.997>.
- [6] C. Boccaccio, P.M. Comoglio, Invasive growth: a MET-drive genetic programme for cancer and stem cells, *Nat. Rev. Cancer* 6 (2006) 637–645, <https://doi.org/10.1038/nrc1912>.
- [7] O. Miranda, M. Farooqui, J.M. Siegfried, Status of Agents Targeting the HGF/c-Met Axis in Lung Cancer, *Cancers* 10 (2018) 280–297, <https://doi.org/10.3390/cancers10090280>.
- [8] O. Firuzi, P.P. Che, B.E. Hassouni, et al., Role of c-MET Inhibitors in Overcoming Drug Resistance in Spheroid Models of Primary Human Pancreatic Cancer and Stellate Cells, *Cancers* 11 (2019) 638–660, <https://doi.org/10.3390/cancers11050638>.

- [9] L. Jia, X. Yang, W. Tian, et al., Increased Expression of c-Met is Associated with Chemotherapy-Resistant Breast Cancer and Poor Clinical Outcome, *Med. Sci. Monit.*, 24 (2018) 8239–8249, <http://doi.org/10.12659/MSM.913514>.
- [10] N. Faham, A.L. Welm, RON Signaling Is a Key Mediator of Tumor Progression in Many Human Cancers, *Cold Spring Harb Symp Quant Biol.* 81 (2016) 177–188, <https://doi.org/10.1101/sqb.2016.81.031377>.
- [11] N.M. Benight, S.E. Waltz, Ron receptor tyrosine kinase signaling as a therapeutic target, *Expert Opin. Ther. Targets* 16 (2012) 921–931, <https://doi.org/10.1517/14728222.2012.710200>.
- [12] M.H. Wang, D. Wang, Y.Q. Chen, Oncogenic and invasive potentials of human macrophage-stimulating protein receptor, the RON receptor tyrosine kinase, *Carcinogenesis* 24 (2003) 1291–1300, <https://doi.org/10.1093/carcin/bgg089>.
- [13] A. Danilkovitch-Miagkova, Oncogenic signaling pathways activated by RON receptor tyrosine kinase, *Curr. Cancer Drug Targets* 3 (2003) 31–40, <https://doi.org/10.2174/1568009033333745>.
- [14] B. Yin, Z. Liu, Y. Wang, et al., RON and c-Met facilitate metastasis through the ERK signaling pathway in prostate cancer cells, *Oncol Rep.* 37 (2017) 3209–3218, <https://doi.org/10.3892/or.2017.5585>.
- [15] J. Wang, A. Rajput, J.L. Kan, et al., Knockdown of Ron kinase inhibits mutant phosphatidylinositol 3-kinase and reduces metastasis in human colon carcinoma, *J Biol. Chem.* 284 (2009) 10912–10922, <https://doi.org/10.1074/jbc.M809551200>.
- [16] J. Logan-Collins, R.M. Thomas, P. Yu, et al., Silencing of RON receptor signaling promotes apoptosis and gemcitabine sensitivity in pancreatic cancers, *Cancer Res.* 70 (2010) 1130–1140, <https://doi.org/10.1158/0008-5472.CAN-09-0761>.
- [17] P.K. Parikh, M.D. Ghate, Recent advances in the discovery of small molecule c-Met Kinase inhibitors, *Eur. J. Med. Chem.* 143 (2018) 1103–1138, <https://doi.org/10.1016/j.ejmech.2017.08.044>.
- [18] Z.G. Sun, Y.A. Yang, Z.G. Zhang, et al., Optimization techniques for novel c-Met kinase inhibitors, *Expert Opinion on Drug Discovery* 14 (2019) 59–69, <https://doi.org/10.1080/17460441.2019.1551355>.
- [19] H. Oliveres, E. Pinda, J. Maurel, MET inhibitors in cancer: pitfalls and challenges, *Expert Opinion on Investigational Drugs* 29 (2019) 73–85, <https://doi.org/10.1080/13543784.2020.1699532>.
- [20] V.L. Keedy, H.J. Lenz, L. Saltz, et al., First-in-human phase I dose escalation study of MK-8033 in patients with advanced solid tumors, *Invest New Drugs* 36 (2018) 860–868, <https://doi.org/10.1007/s10637-018-0567-z>.
- [21] A.R. He, R.B. Cohen, C.S. Denlinger, et al., First-in-Human Phase I Study of Merestinib, an Oral Multikinase Inhibitor, Patients with Advanced Cancer. *The Oncologist* 24 (2019) e930–e942, <https://doi.org/10.1634/theoncologist.2018-0411>.
- [22] B. Qi, Y. Yang, G. Gong, et al., Discovery of N^1 -(4-((7-(3-(4-ethylpiperazin-1-yl)propoxy)-6-methoxyquinolin-4-yl)oxy)-3,5-difluorophenyl)- N^3 -(2-(2,6-difluorophenyl)-4-oxothiazolidin-3-yl)urea as a multi-tyrosine kinase inhibitor for drug-sensitive and drug-resistant cancers treatment, *Eur. J. Med. Chem.* 163 (2019) 10–27, <https://doi.org/10.1016/j.ejmech.2018.11.057>.
- [23] B. Qi, Y. Yang, H. He, et al., Identification of novel N^1 -(2-aryl-1,3-thiazolidin-4-one)- N^3 -aryl ureas showing potent multi-tyrosine kinase inhibitory activities, *Eur. J. Med. Chem.* 146 (2018) 368–380, <https://doi.org/10.1016/j.ejmech.2018.01.061>.
- [24] I. Szabadkai, R. Torka, R. Garamvölgyi, et al., Discovery of N -[4-(Quinolin-4-yloxy)phenyl]benzenesulfonamides as Novel AXL Kinase Inhibitors, *J. Med. Chem.* 61 (2018) 6277–6292, <https://doi.org/10.1021/acs.jmedchem.8b00672>.
- [25] L. Pisani, R.M. Lacobazzi, M. Catto, et al., Investigating alkyl nitrates as nitric oxide releasing precursors of multitarget acetylcholinesterase-monoamine oxidase B inhibitors, *Eur. J. Med. Chem.* 161 (2019) 292–309.
- [26] J.J. Cui, Targeting receptor tyrosine kinase MET in cancer: small molecule inhibitors and clinical progress, *J. Med. Chem.* 57 (2014) 4427–4453, <https://doi.org/10.1021/jm401427c>.
- [27] B. Qi, X. Xu, Y. Yang, et al., Discovery of thiazolidin-4-one urea analogues as novel multikinase inhibitors that potently inhibit FLT3 and VEGFR2, *Bioorg. Med. Chem.* 27 (2019) 2127–2139, <https://doi.org/10.1016/j.bmc.2019.03.049>.